

Introduction of a Mesityl Substituent on Pyridyl Rings as a Facile Strategy for Improving the Performance of Luminescent 1,3-Bis-(2-pyridyl)benzene Platinum(II) Complexes: a Springboard for Blue OLEDs[†]

Alessia Colombo,^a Giulia De Soricellis,^{a, b} Claudia Dragonetti,^a Francesco Fagnani,^{*, a} Dominique Roberto,^a Bertrand Carboni,^c Véronique Guerchais,^c Thierry Roisnel,^c Massimo Cocchi,^d Simona Fantacci,^e Eros Radicchi,^{e, f} and Daniele Marinotto^g

^a Dipartimento di Chimica dell'Università degli Studi di Milano and UdR-INSTM di Milano, Via C. Golgi 19, I-20133 Milano, Italy. E-mail: francesco.fagnani@unimi.it

^b Dipartimento di Chimica, Università di Pavia, Via Taramelli 12, I-27100 Pavia, Italy.

^c Université de Rennes 1, CNRS, ISCR (Institut des Sciences Chimiques de Rennes) - UMR 6226, F-35000 Rennes, France.

^d Istituto per la Sintesi Organica e la Fotoreattività (ISOF), Consiglio Nazionale delle Ricerche (CNR), via P. Gobetti 101, I-40129 Bologna, Italy.

^e Istituto di Scienze e Tecnologie Chimiche "Giulio Natta" SCITEC, Consiglio Nazionale delle Ricerche (CNR), Computational Laboratory for Hybrid/Organic Photovoltaics (CLHYO), via Elce di Sotto 8, I-06213, Perugia, Italy.

^f NRG - Dipartimento di Biotecnologie, Università degli Studi di Verona e INSTM, RU di Verona, Strada le Grazie 15, I-37134 Verona, Italy.

^g Istituto di Scienze e Tecnologie Chimiche "Giulio Natta" (SCITEC), Consiglio Nazionale delle Ricerche (CNR), via C. Golgi 19, I-20133 Milano, Italy.

Contents

I. General Information	2
II. Synthesis of [Pt(bis(4-Mes-py)-4,6-dFb)Cl]	3
III. X-ray diffraction data	5
IV. ¹ H, ¹³ C and ¹⁹ F NMR spectra.....	8
V. Photophysical data in solution and at the solid state.....	12
VI. DFT and TDDFT data	24
VII. OLEDs fabrication	36
VIII. References.....	37

I. General Information

Unless otherwise noted, solvents (dioxane, 1,2-dimethoxyethane and acetonitrile) and all commercially available chemicals were used without further purification. Anhydrous toluene was obtained through distillation over sodium/benzophenone. Air- and water-sensitive reactions were performed in flame-dried glasswares under argon atmosphere. For oxygen sensitive reaction, when specified, solvent was degassed prior to use by slow bubbling of argon. ¹H NMR spectra (300, 400 or 500 MHz), ¹³C NMR (75, 101 or 126 MHz), ¹¹B (128 MHz) and ¹⁹F (376 MHz) were recorded on Bruker AC 300 and AC 400 spectrometers. Chemical shifts δ are given in ppm and coupling constants J in Hz. Multiplicities are presented as follows: s = singlet, d = doublet, t = triplet, q = quartet, m = multiplet, br = broad. High-resolution mass spectra (HRMS) were recorded, either on a Bruker MaXis 4G, an Agilent 6510, or a Thermo Fisher Q-Exactive spectrometer (Centre Régional de Mesures Physiques de l’Ouest, Rennes) using positive or negative ion Electron-Spray ionization techniques (respectively ESI+, ESI-). IR spectrum was recorded on a 100 FT-IR Perkin-Elmer spectrometer. Purifications by silica gel chromatography were carried out on silica 0.060-0.200 mm, 60 Å. Flash chromatography were performed on a Grace Reveleris™ apparatus. Analytical thin layer chromatography was performed on Merck Silica Gel 60 F254 plates. The structure’s parameters were determined performing the X-ray analysis using a D8 VENTURE Bruker AXS diffractometer, Mo-K α radiation ($\lambda = 0.71073 \text{ \AA}$), T = 150 K. Elemental analyses were performed by the Centre Regional de Mesures Physiques de l’Ouest, University of Rennes 1.

II. Synthesis of [Pt(bis(4-Mes-py)-4,6-dFb)Cl]

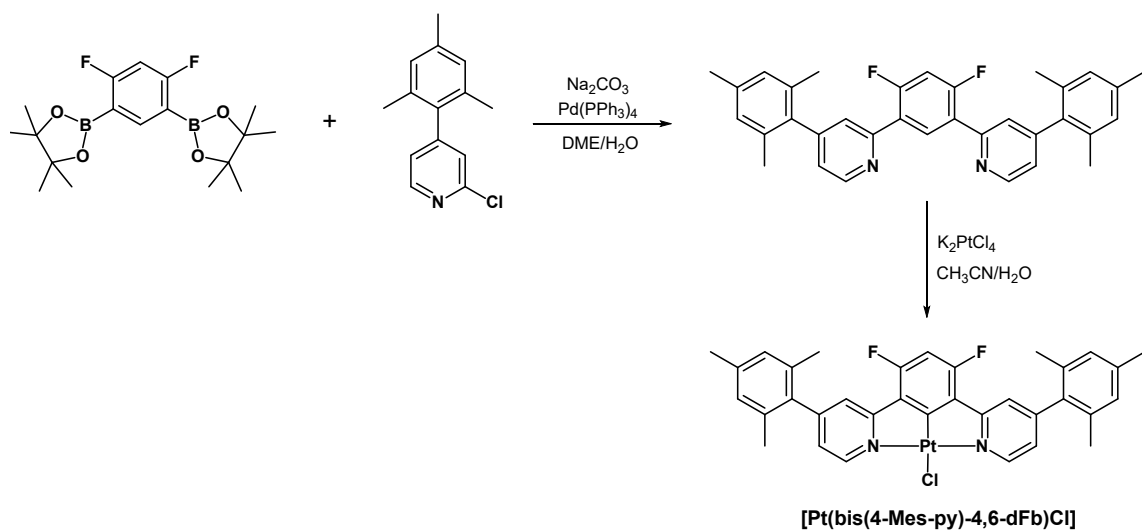


Figure S1. Synthetic pathway followed for the preparation of [Pt(bis(4-Mes-py)-4,6-dFb)Cl].

2,2'-(4,6-difluoro-1,3-phenylene)bis(4-mesitylpyridine). 2-chloro-4-mesitylpyridine^[1] (0.30 g, 1.3 mmol), 2,2'-(4,6-difluoro-1,3-phenylene)bis(4,4,5,5-tetramethyl-1,3,2-dioxaborolane)^[2] (0.21 g, 0.6 mmol), an aqueous solution of Na₂CO₃ (1 M, 7.0 mL) were placed in a two neck round bottom flask filled with argon. Then, 7.0 mL of DME were added and the solution was purged by bubbling the argon for 30 min before adding Pd(PPh₃)₄ (0.11 g, 0.1 mmol). The flask was sealed and the reaction mixture was heated at 100°C for 24h. After addition of dichloromethane (20 mL) and water (5 mL), the two layers were separated and the aqueous one was extracted with dichloromethane (2 x 20 mL). The combined organic phases were washed with brine, dried over anhydrous MgSO₄ and concentrated *in vacuo*. The residue was purified by silica gel column chromatography (cyclohexane:AcOEt, 10:0 to 7:3, v/v) to give a yellow oil (0.20 g, 70% yield).

¹H NMR (300 MHz, CDCl₃, δ): 8.79 (d, *J* = 4.9 Hz, 2H), 8.72 (t, *J* = 8.9 Hz, 1H), 7.62 (s, 2H), 7.12 (dd, *J* = 1.5 and 5.0 Hz, 2H), 7.03 (t, *J* = 10.6 Hz, 1H), 7.00 (s, 4H), 2.37 (s, 6H), 2.08 (s, 12H). ¹⁹F {1H} NMR (282.36 MHz, CDCl₃, δ): -113.27 (s, 2F). ¹³C {1H} NMR (75.48 MHz, CDCl₃, δ): 160.5 (dd, *J* = 255.5 and 12.4 Hz), 152.7, 150.00, 149.95, 137.6, 136.2, 135.2, 133.8 (t, *J* = 4.2 Hz), 128.4, 125.4 (t, *J* = 4.3 Hz), 124.7 (dd, *J* = 9.8 and 6.1 Hz), 123.6, 104.9 (t, *J* = 27.1 Hz), 21.0, 20.6. HRMS (ESI+): (M + H)⁺ calcd for C₃₄H₃₁N₂F₂, 505.2449; found: 505.2450.

[Pt(bis(4-Mes-py)-4,6-dFb)Cl]. According to the literature,^[2] in a Schlenk tube under an argon atmosphere, 2,2'-(4,6-difluoro-1,3-phenylene)bis(4-mesitylpyridine) (0.20 g, 0.4 mmol) was dissolved in 4.5 mL of acetonitrile. In parallel, K₂PtCl₄ (0.34 g, 0.8 mmol) was solubilized into 0.5

mL of water under ultrasound sonication and then added to the reaction mixture. The solution was degassed by bubbling argon directly in the mixture for 40 min. The mixture was then stirred at reflux at 110°C for 3 days, until it became a yellow suspension. Upon cooling to ambient temperature, the reaction mixture was filtered through a 0.45 µm Nylon membrane. The isolated yellow solid was washed with water, diethylether and dried under vacuum. (88 mg, 30% yield). ^1H NMR (300 MHz, CDCl_3 , δ): 9.42 (dd, $J = 0.7$ and 5.9 Hz, $^3J(^{195}\text{Pt}) = 40.4$ Hz, 2H), 7.81-7.76 (m, 2H), 7.17 (dd, $J = 1.9$ and 4.0 Hz, 2H), 7.03 (s, 4H), 6.73 (t, $J = 11.2$ Hz, 1H), 2.38 (s, 6H), 2.11 (s, 12H). ^{19}F {1H} NMR (282.36 MHz, CDCl_3 , δ): -107.90 (s, $^4J(^{195}\text{Pt}) = 54.4$ Hz, 2F). ^{13}C {1H} NMR (75.48 MHz, CDCl_3 , δ): 164.3, 154.1, 151.9, 138.4, 135.1, 134.8, 128.7, 124.5, 123.7, 99.4, 29.7, 21.1, 20.6 (The ^{13}C NMR spectrum could not be analyzed accurately, the peaks corresponding to certain carbons are not visible). Anal. calcd. for $\text{C}_{36}\text{H}_{33}\text{Cl}_5\text{F}_2\text{N}_2\text{Pt}$, 2 CH_2Cl_2 : C, 47.83; H, 3.68; N, 3.10; found: C, 47.64; H, 3.64; N, 3.05.

III. X-ray diffraction data

2,2'-(4,6-Difluoro-1,3-phenylene)bis(4-mesityl pyridine)

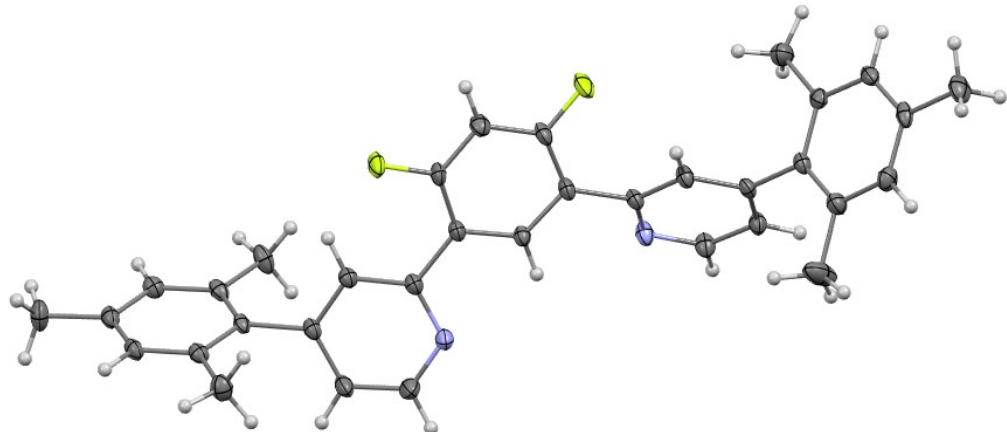


Figure S2. Thermal ellipsoids are shown at the 50% probability level.

CCDC number: 2087751	
Empirical formula	C ₃₄ H ₃₀ F ₂ N ₂
Formula weight	504.60 g/mol
Temperature	150 K
Wavelength	0.71073 Å
Crystal system, space group	triclinic, P -1
Unit cell dimensions	a = 11.3192(8) Å, α = 101.018(3)
	b = 11.4478(9) Å, β = 108.967(3)
	c = 11.6150(10) Å, γ = 100.767(3)
Volume	1345.94(19) Å ³
Z	4
Calculated density	1.245 g.cm ⁻³
Absorption coefficient	0.082 mm ⁻¹
F(000)	532
Crystal size	0.490 x 0.190 x 0.120 mm
Theta range for data collection	2.183 to 27.546
Limiting indices	-14 ≤ h ≤ 13, -14 ≤ k ≤ 14, -0 ≤ l ≤ 15
Reflections collected / unique	6088 / 6088 [R(int) ^a = 0.0834]
Reflections [I>2σ]	4920
Completeness to theta = 75.47	0.981
Absorption correction	Multi-scan
Max. and min. transmission	0.990, 0.961
Refinement method	Full-matrix least-squares on F ²
Data / restraints / parameters	6088 / 0 / 349

Goodness-of-fit on F^2	1.113
Final R indices [$I > 2\sigma(I)$]	$R1^c = 0.0784$, $wR2^d = 0.2065$
R indices (all data)	$R1^c = 0.0942$, $wR2^d = 0.2182$
Largest diff. peak and hole	0.484 d -0.382 e $\cdot\text{\AA}^{-3}$

[Pt(bis(4-Mes-py)-4,6-dFb)Cl]

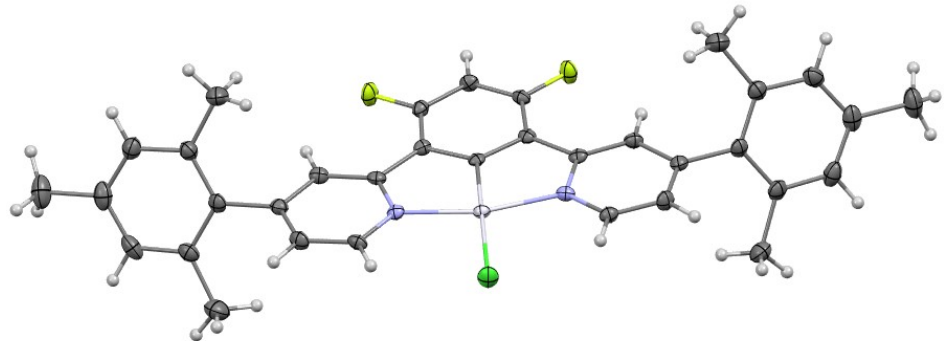
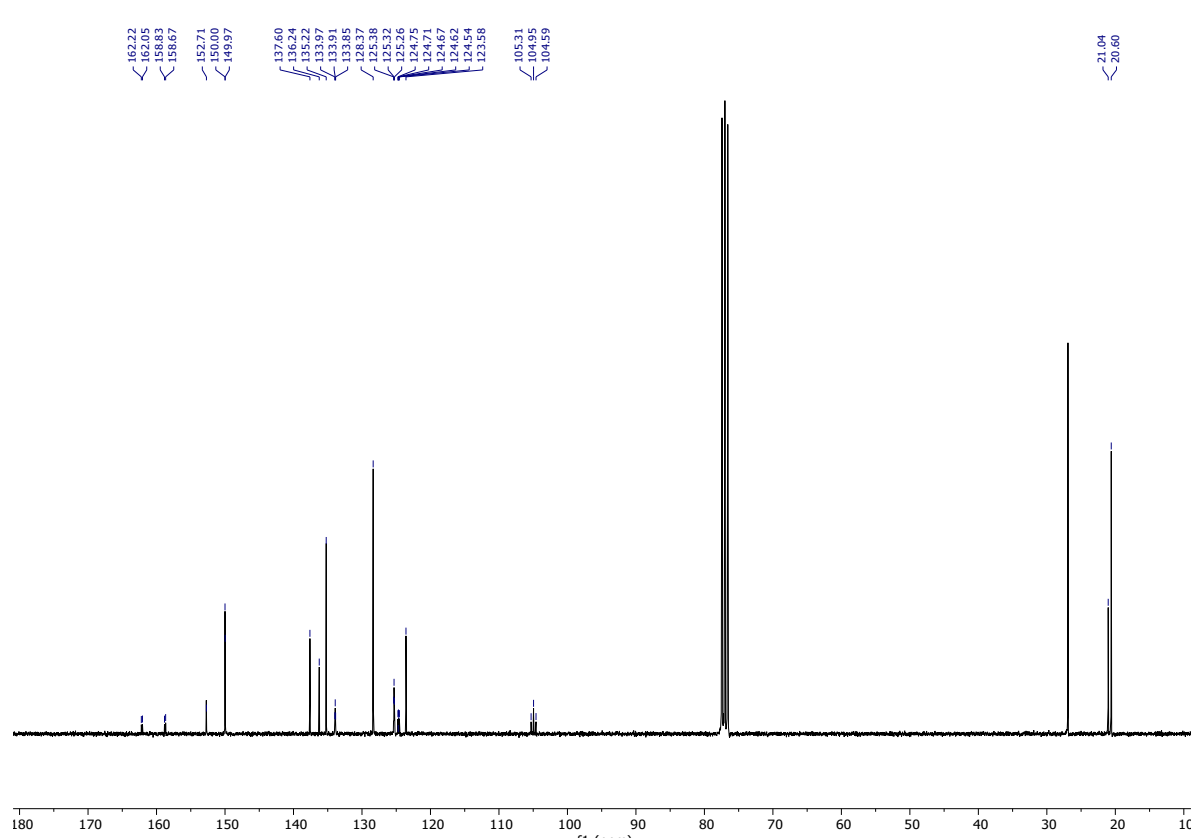
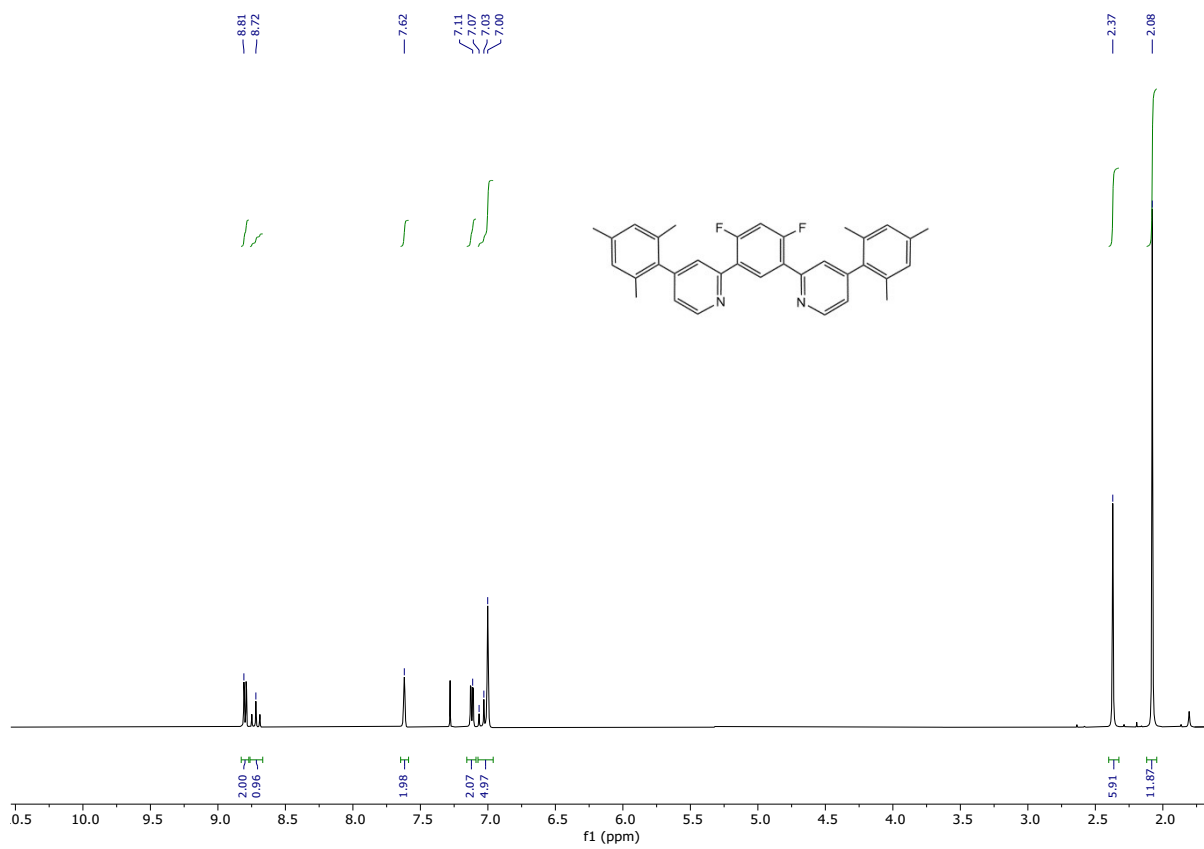


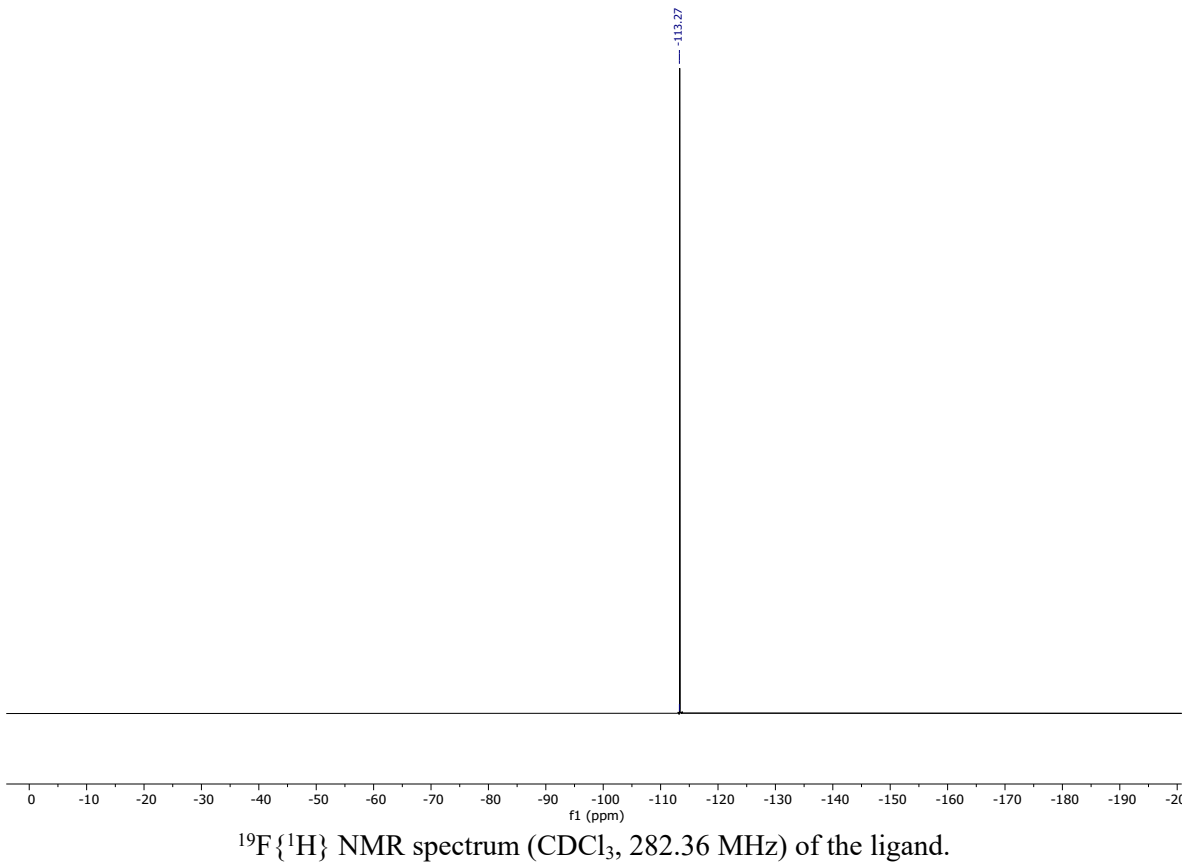
Figure S3. Thermal ellipsoids are shown at the 50% probability level (solvent molecules not shown).

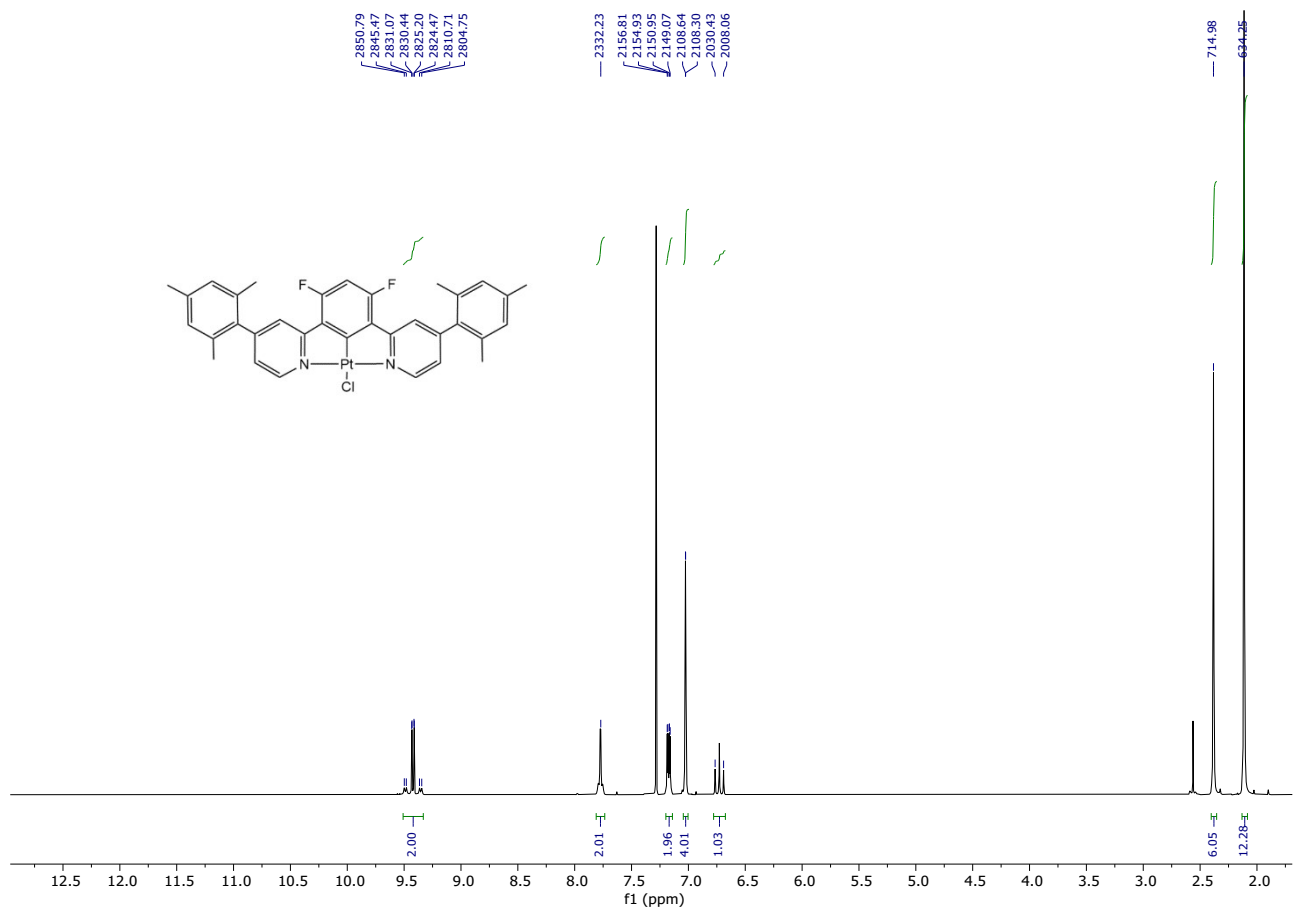
CCDC number: 2087750	
Empirical formula	C ₃₄ H ₂₉ ClF ₂ N ₂ Pt•2(CH ₂ Cl ₂)
Formula weight	903.98 g/mol
Temperature	150 K
Wavelength	0.71073 Å
Crystal system, space group	Orthorhombic, P b c a
Unit cell dimensions	a = 32.569(3) Å, α = 90
	b = 6.6720(6) Å, β = 90
	c = 33.849(3) Å, γ = 90
Volume	7355.2(12) Å ³
Z	8
Calculated density	1.633 g.cm ⁻³
Absorption coefficient	4.217 mm ⁻¹
F(000)	3552
Crystal size	0.480 x 0.300 x 0.15 mm
Theta range for data collection	2.501 to 27.508
Limiting indices	-42 ≤ h ≤ 42, -8 ≤ k ≤ 8, -43 ≤ l ≤ 39
Reflections collected / unique	55960 / 8431 [R(int) ^a = 0.0394]
Reflections [$I > 2\sigma$]	7255
Completeness to theta max	0.996
Absorption correction	Multi-scan
Max. and min. transmission	0.531, 0.278

Refinement method	Full-matrix least-squares on F^2
Data / restraints / parameters	8431 / 0 / 421
Goodness-of-fit on F^2	1.103
Final R indices [$I > 2\sigma(I)$]	$R1^c = 0.0323, wR2^d = 0.0684$
R indices (all data)	$R1^c = 0.0417, wR2^d = 0.0723$
Largest diff. peak and hole	1.517 and -1.306 e \cdot Å $^{-3}$

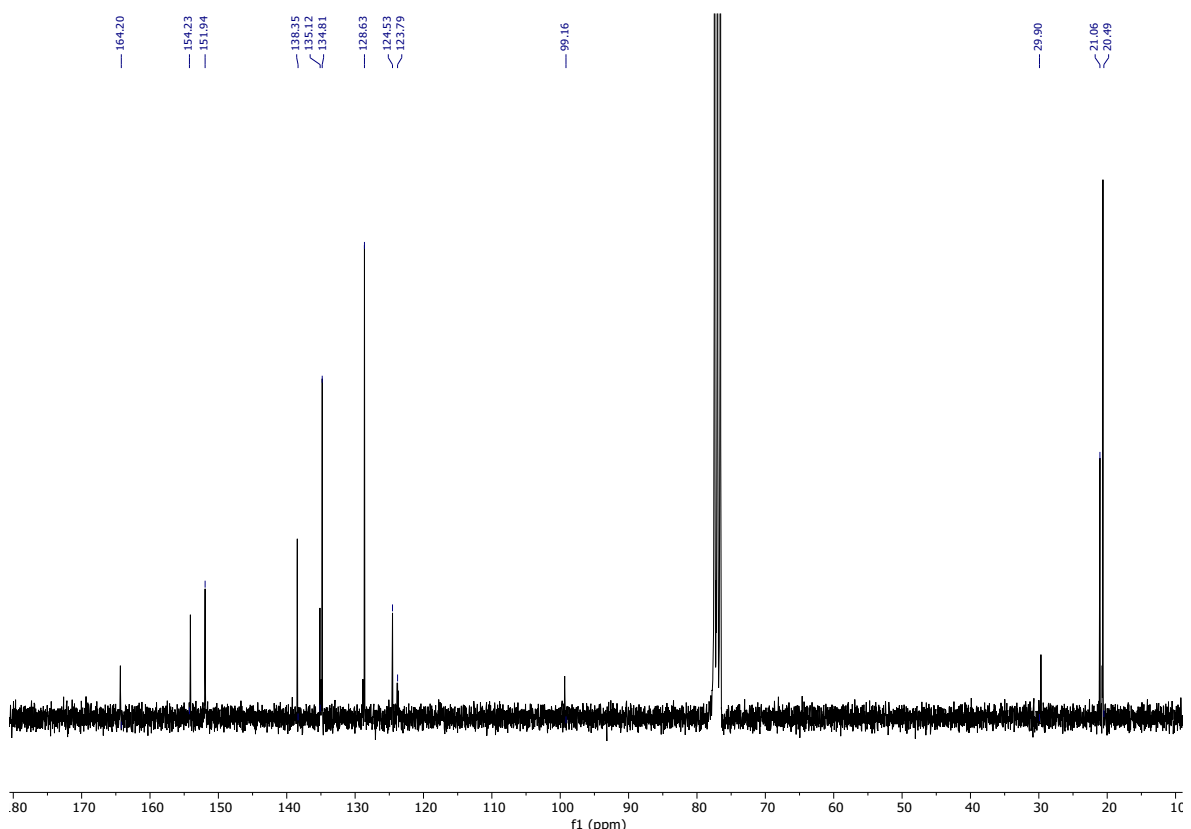
IV. ^1H , ^{13}C and ^{19}F NMR spectra



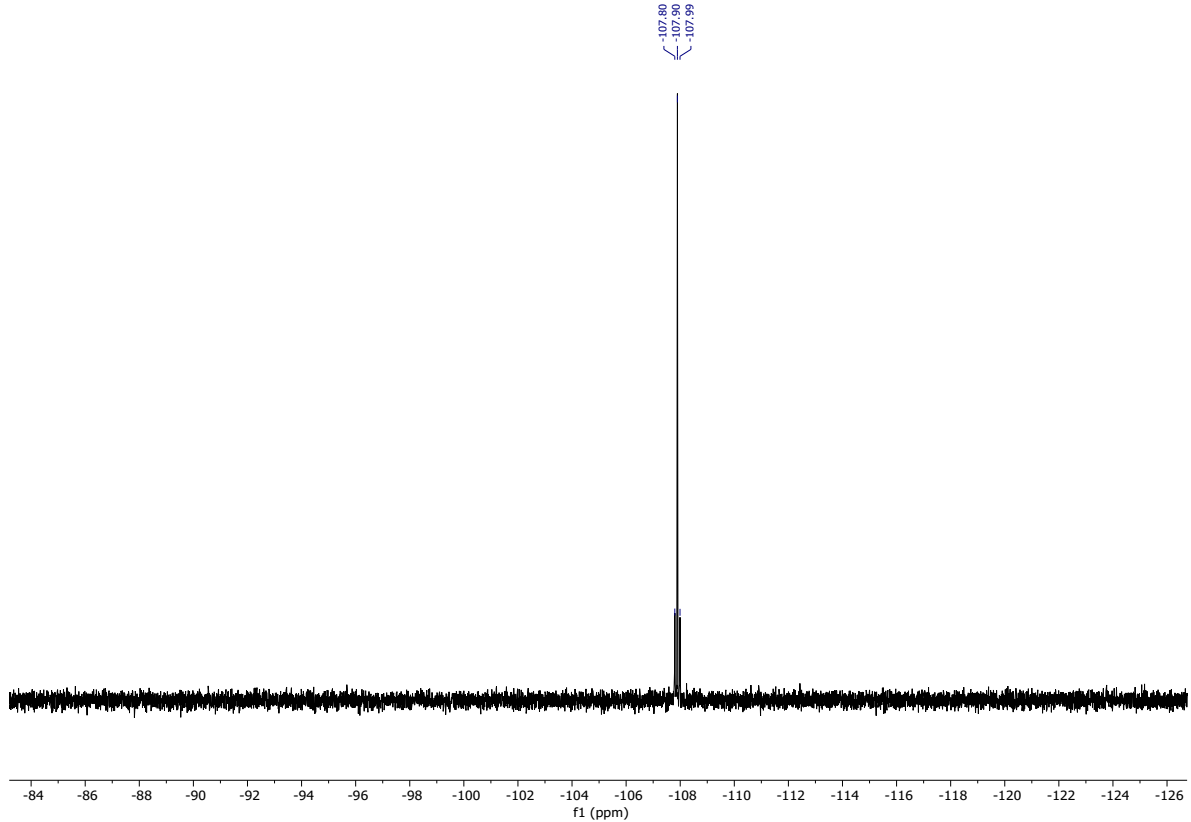




¹H NMR spectrum (CDCl_3 , 300 MHz) of the Pt(II) complex.



$^{13}\text{C}\{^1\text{H}\}$ NMR spectrum (CDCl_3 , 75 MHz) of the Pt(II) complex.



$^{19}\text{F}\{^1\text{H}\}$ NMR spectrum (CDCl_3 , 282.36 MHz) of the Pt(II) complex.

V. Photophysical data in solution and at the solid state

Luminescence measurements

Luminescence measurements were carried out in CH₂Cl₂ solution after bubbling with nitrogen through the solvent for 5 minutes in order to remove dissolved oxygen.

Absolute photoluminescence quantum yield (Φ) for a solution or thin film was measured using a C11347 Quantaurus Hamamatsu Photonics K.K spectrometer. A description of the experimental setup and measurement method can be found in the article of K. Suzuki *et al* [3]. Φ was calculated through Equation:

$$\Phi = \frac{PN(Em)}{PN}$$

where PN(Em) is the number of emitted photons, PN(Abs) the number of absorbed photons, λ the wavelength, h the Planck's constant, c the speed of light, I_{em}^{sample} and $I_{em}^{reference}$ the photoluminescence intensities of the sample and reference, I_{exc}^{sample} and $I_{exc}^{reference}$ the excitation light intensities of the sample and reference. PN(Em) is calculated in the wavelength interval $[\lambda_i, \lambda_f]$, where λ_i is taken at about 10 nm above the excitation wavelength, while λ_f is the upper end wavelength in the emission spectrum. The error made was estimated at around 5%.

Steady state and time-resolved fluorescence data were obtained using a FLS980 spectrofluorimeter (Edinburgh Instrument Ltd). Emission spectra were corrected for background intensity and quantum efficiency of the photomultiplier tube. Excitation spectra were corrected for the intensity fluctuation of a 450 W Xenon arc lamp. Quartz cuvettes with 1 cm optical path length were used for diluted solutions, meanwhile quartz cuvettes of 2 mm optical path length were used for concentrated solutions to avoid the inner filter effect.

Time-resolved fluorescence measurements were performed through the time-correlated single photon counting technique with an Edinburgh Picosecond Pulsed Diode Laser (emitted wavelength 374 nm) or a pulsed Xenon arc lamp. Moreover, time-resolved fluorescence curves were fitted using a multi-exponential function:

$$I(\lambda, t) = \sum_{i=1}^m \alpha_i(\lambda) \exp\left(-\frac{t}{\tau_i}\right)$$

where m is the number of exponentials, $\alpha_i(\lambda)$ is the amplitude at wavelength λ and τ_i is the lifetime of the component i . The quality of the fit was evaluated through the reduced χ^2 values.

In case of multi-exponential decay, it is possible define an average lifetime as:

$$\tau_{\text{av}} = \frac{\sum_{n=1}^m \alpha_n \tau_n^2}{\sum_{n=1}^m \alpha_n \tau_n}, \quad m = \text{multi-exponential decay number of the fit.}$$

Absorption vs Concentration

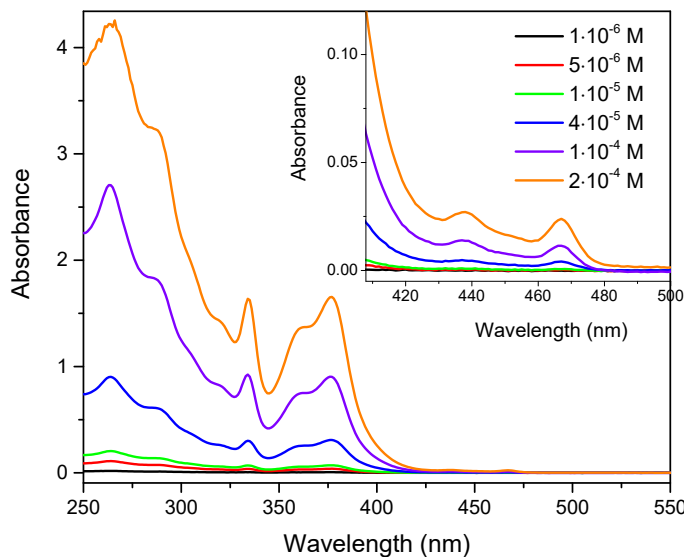
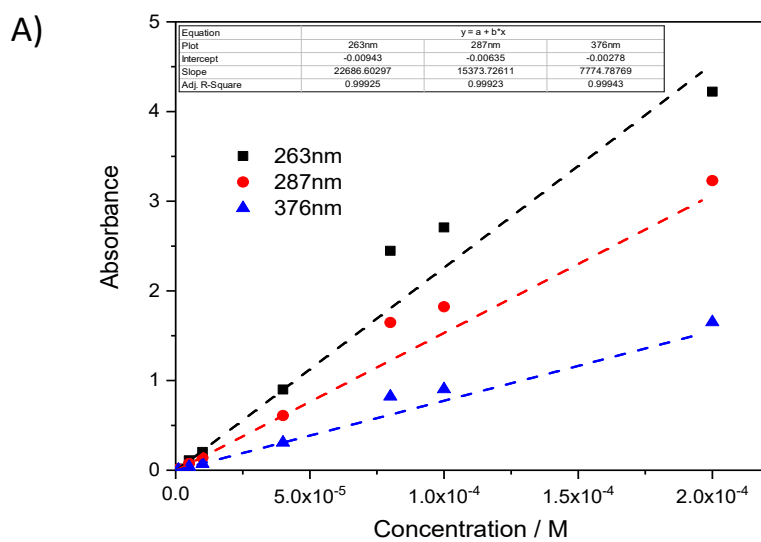


Figure S4. Absorption spectra of **[Pt(bis(4-Mes-py)-4,6-dFb)Cl]** in CH_2Cl_2 at different concentrations. The weak bands at longer wavelengths are shown on an expanded scale for clarity.



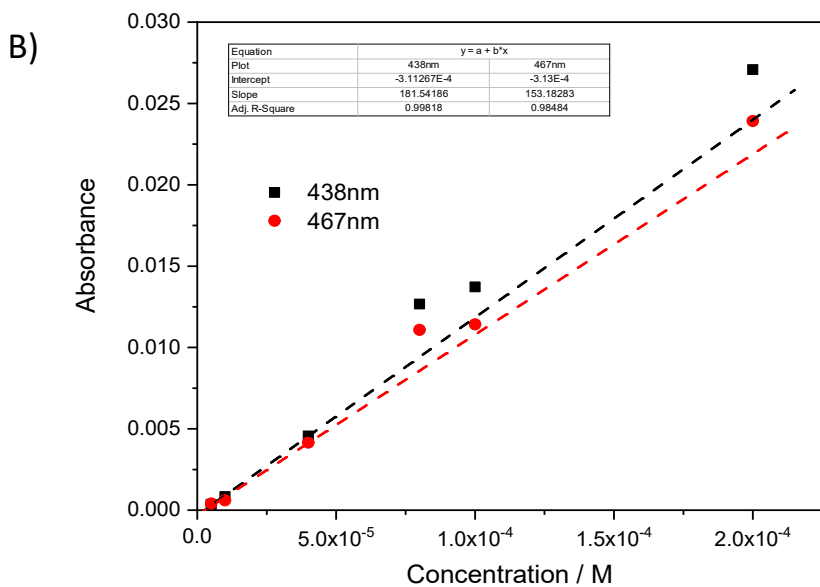


Figure S5. Panels A and B: Absorbance vs Concentration for **[Pt(bis(4-Mes-py)-4,6-dFb)Cl]** in CH_2Cl_2 at different wavelengths. The Lambert-Beer law is no longer valid at high concentrations and the linear fit is applied up to $4 \cdot 10^{-5}$ M.

Table S1. Molar extinction coefficient (ϵ) of **[Pt(bis(4-Mes-py)-4,6-dFb)Cl]** in CH_2Cl_2 .

	263 nm	287 nm	376 nm	438 nm	467 nm
$\epsilon / \text{M}^{-1} \text{ cm}^{-1}$	$2.3 \cdot 10^4$	$1.5 \cdot 10^4$	$7.8 \cdot 10^3$	$1.8 \cdot 10^2$	$1.5 \cdot 10^2$

Excitation spectra

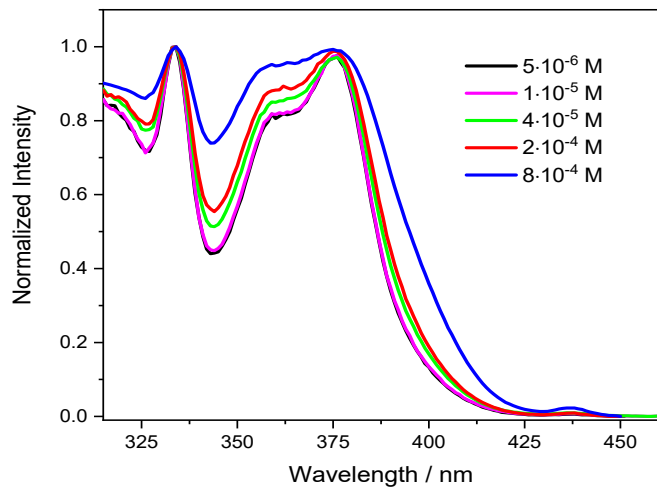


Figure S6. Excitation spectra of $[\text{Pt}(\text{bis}(4\text{-Mes-py})\text{-4,6-dFb})\text{Cl}]$ in CH_2Cl_2 at different concentrations, emission wavelength 471 nm.

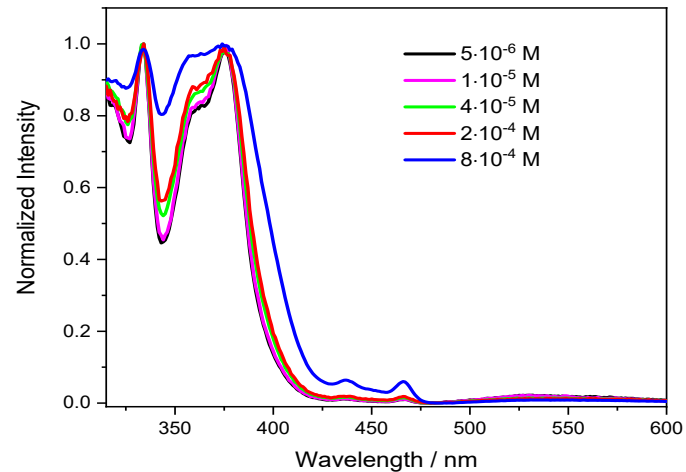


Figure S7. Excitation spectra of $[\text{Pt}(\text{bis}(4\text{-Mes-py})\text{-4,6-dFb})\text{Cl}]$ in CH_2Cl_2 at different concentrations, emission wavelength 680 nm.

Excited state decay measurement and relative fit at different concentrations

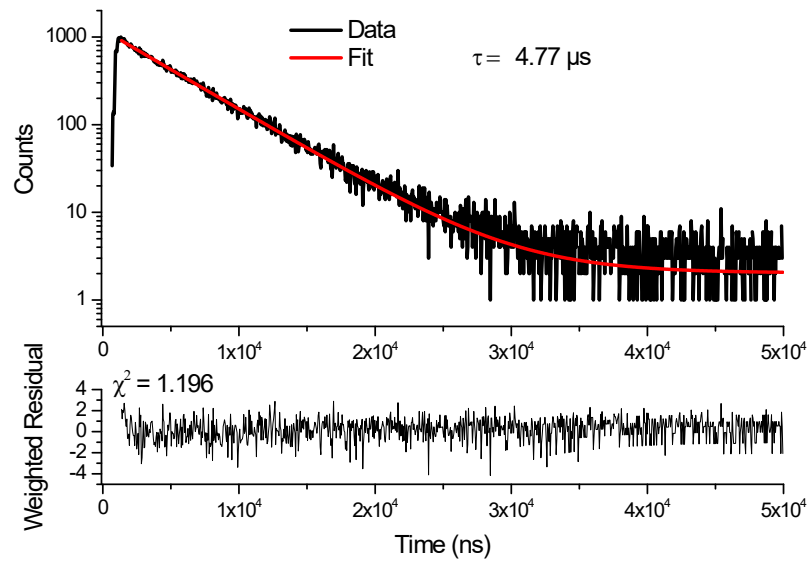


Figure S8. Excited state decay measurement of **[Pt(bis(4-Mes-py)-4,6-dFb)Cl]** in CH_2Cl_2 at $5 \cdot 10^{-6}$ M, emission wavelength 471 nm, excitation wavelength 374 nm.

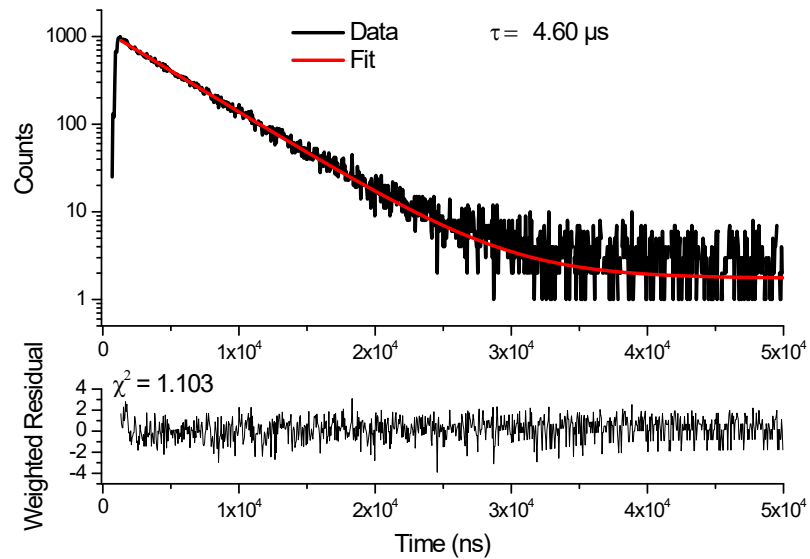


Figure S9. Excited state decay measurement of **[Pt(bis(4-Mes-py)-4,6-dFb)Cl]** in CH_2Cl_2 at $1 \cdot 10^{-5}$ M, emission wavelength 471 nm, excitation wavelength 374 nm.

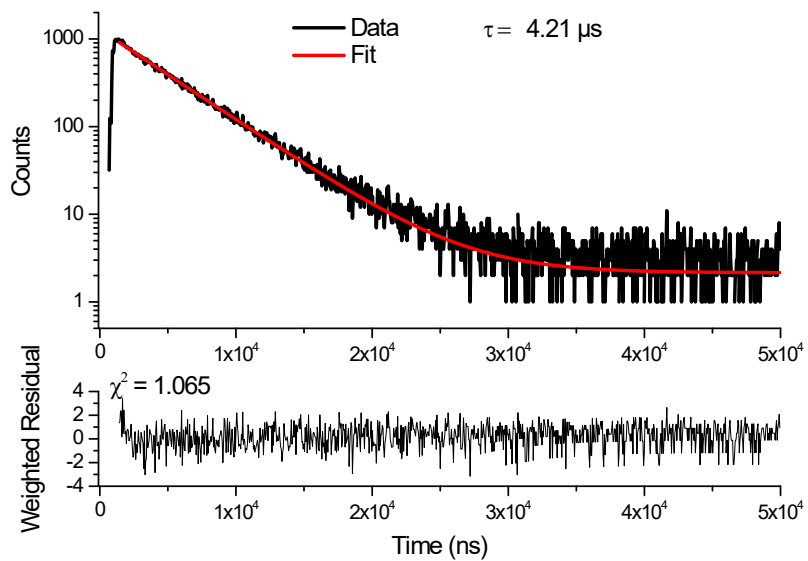


Figure S10. Excited state decay measurement of **[Pt(bis(4-Mes-py)-4,6-dFb)Cl]** in CH_2Cl_2 at $4 \cdot 10^{-5}$ M, emission wavelength 471 nm, excitation wavelength 374 nm.

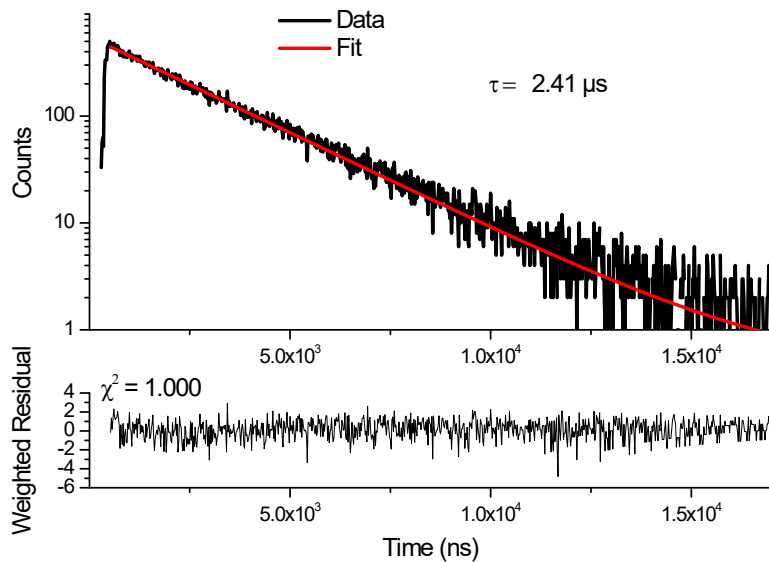


Figure S11. Excited state decay measurement of **[Pt(bis(4-Mes-py)-4,6-dFb)Cl]** in CH_2Cl_2 at $2 \cdot 10^{-4}$ M, emission wavelength 471 nm, excitation wavelength 374 nm.

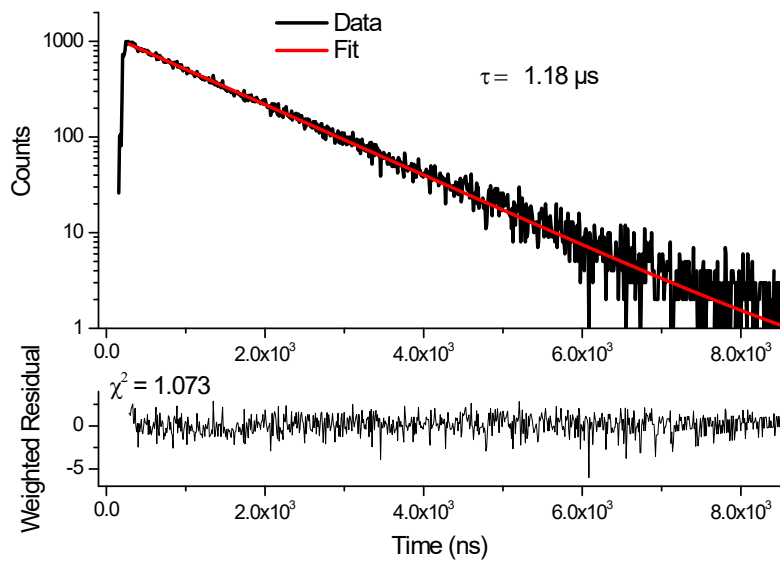


Figure S12. Excited state decay measurement of **[Pt(bis(4-Mes-py)-4,6-dFb)Cl]** complex in CH_2Cl_2 at $8 \cdot 10^{-4}$ M, emission wavelength 471 nm, excitation wavelength 374 nm.

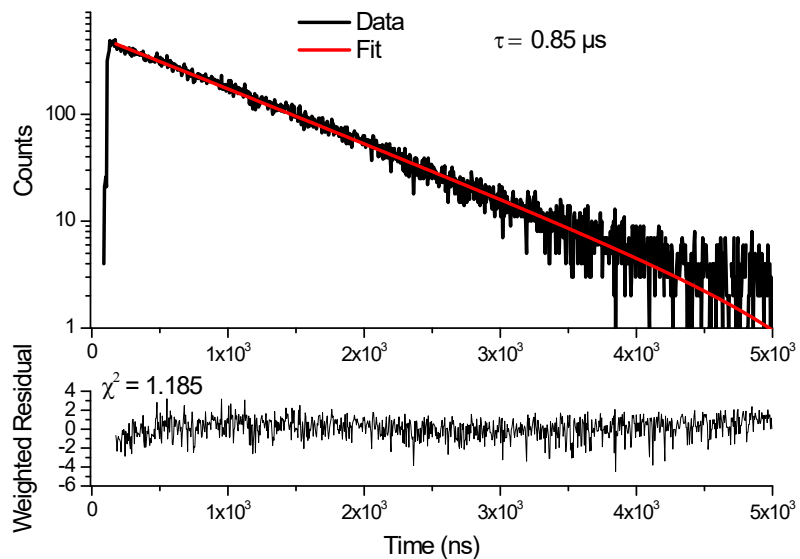


Figure S13. Excited state decay measurement of **[Pt(bis(4-Mes-py)-4,6-dFb)Cl]** in CH_2Cl_2 at $1 \cdot 10^{-3}$ M, emission wavelength 471 nm, excitation wavelength 374 nm.

Table S2. Lifetime: $\lambda_{\text{ex}} = 374 \text{ nm}$, $\lambda_{\text{em}} = 471 \text{ nm}$.

Concentration / M	$5 \cdot 10^{-6}$	$1 \cdot 10^{-5}$	$4 \cdot 10^{-5}$	$2 \cdot 10^{-4}$	$8 \cdot 10^{-4}$	$1.31 \cdot 10^{-3}$
$\tau/\mu\text{s}$	4.77	4.60	4.21	2.41	1.18	0.85

Preparation and characterization of thin films of **[Pt(bis(4-Mes-py)-4,6-dFb)Cl]**

Thin film containing 1 wt % of **[Pt(bis(4-Mes-py)-4,6-dFb)Cl]** in poly-methylmethacrylate (PMMA, $\overline{M}_w \approx 15000$ g/mol) on quartz plate (thickness 1 mm) were obtained by spin-coating (Cookson Electronic Company P-6708D). The solution was prepared with 4.15 mg of complex and 415 mg of PMMA in 3.12 ml of dichloromethane (density 1.33 gr/ml). The parameters of spinning (RPM-revolutions per minute) were RPM 1: 800; Ramp 1: 1 s, Time 1: 5 s; RPM 2: 2000; Ramp 2: 1 s, Time 2: 60 s. Neat thin film was prepared by physical vapor deposition technique

The thickness was measured by an α -step stylus profilometer (DektaK XT, Bruker) obtaining a value of 2.49 ± 0.20 μm and 50 ± 4 nm for the blend PMMA and neat thin films, respectively.

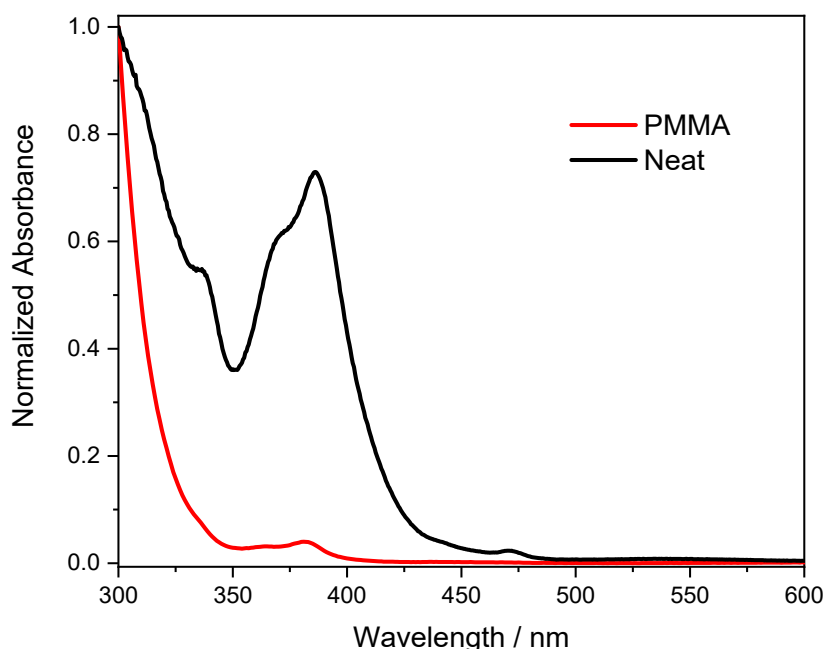


Figure S14. Normalized absorption spectra of **[Pt(bis(4-Mes-py)-4,6-dFb)Cl]** in PMMA and as neat thin film.

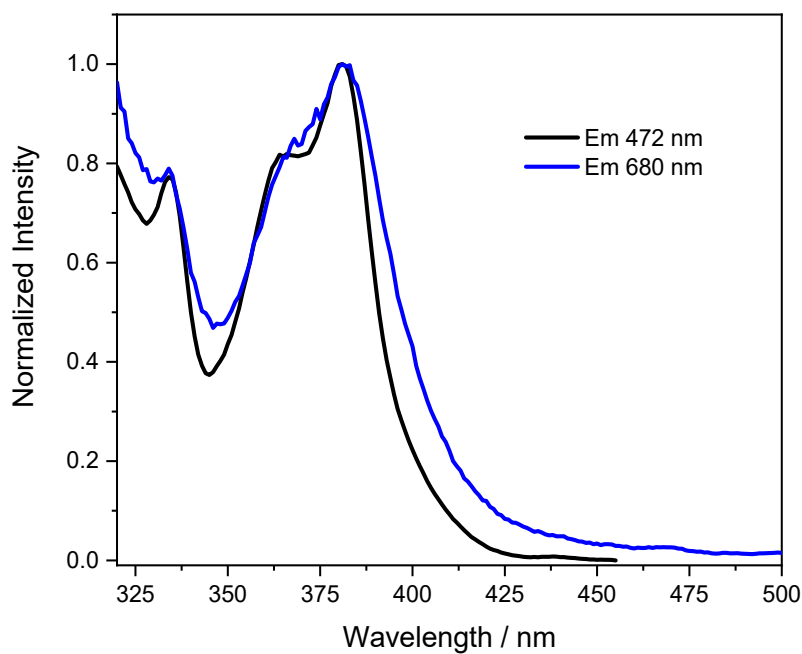


Figure S15. Normalized excitation spectra of **[Pt(bis(4-Mes-py)-4,6-dFb)Cl]** in PMMA thin film.

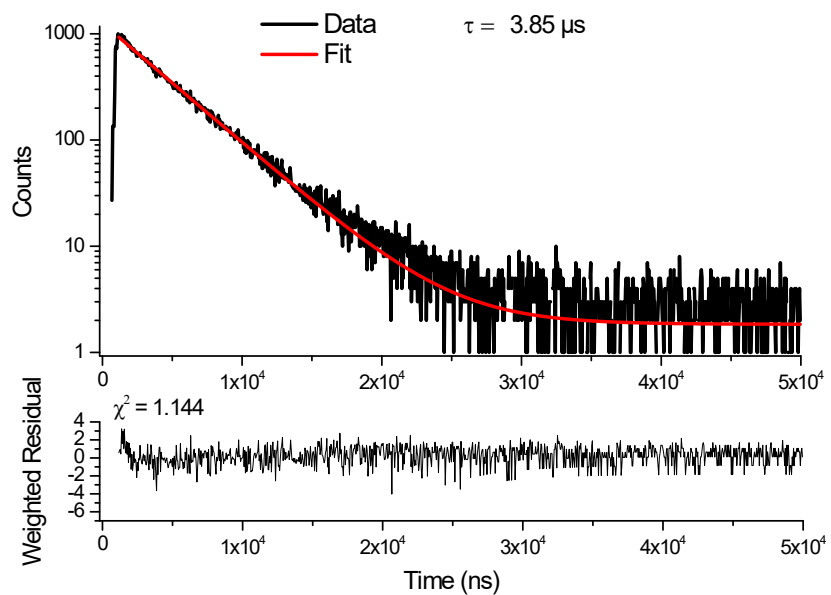


Figure S16. Excited state decay measurement of the PMMA thin film of **[Pt(bis(4-Mes-py)-4,6-dFb)Cl]**, emission 471 nm, excitation 374 nm.

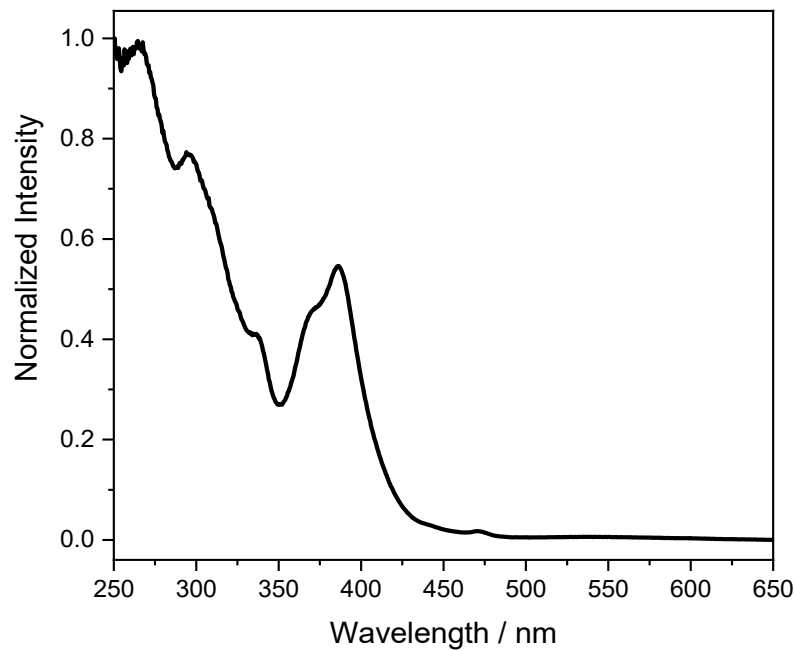


Figure S17. Normalized excitation spectrum of **[Pt(bis(4-Mes-py)-4,6-dFb)Cl]** as neat thin film, emission wavelength 671 nm.

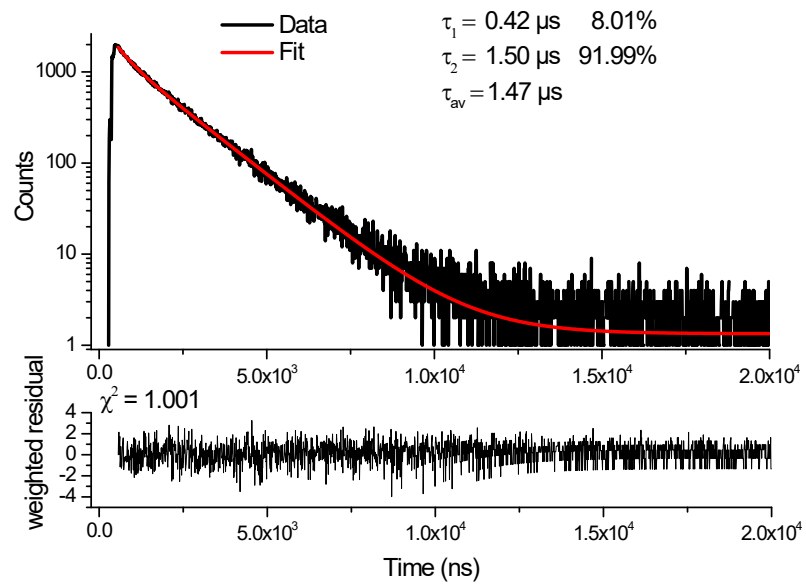


Figure S18. Excited state decay measurement of the neat thin film of **[Pt(bis(4-Mes-py)-4,6-dFb)Cl]**, emission wavelength 671 nm, excitation wavelength 374 nm.

VI. DFT and TDDFT data

Optimized coordinates

[Pt(bis(4-Mes-py)-4,6-dFb)Cl] (B3LYP/6-31G**/CPCM-CH₂Cl₂)

69

6	1.282299	-0.915290	-3.782528
6	0.856673	-0.704500	-2.473266
7	0.777661	0.578167	-1.974654
6	1.110036	1.619976	-2.753184
6	1.534583	1.454120	-4.064410
6	1.625817	0.164833	-4.603138
6	0.456681	-1.735371	-1.511018
6	0.406022	-3.125474	-1.653105
6	-0.009921	-3.960060	-0.617728
6	-0.389907	-3.395038	0.598013
6	-0.367424	-2.013597	0.813929
6	0.062437	-1.224259	-0.264462
6	-0.728978	-1.241015	2.006067
6	-1.188034	-1.754490	3.217198
6	-1.502666	-0.899413	4.278525
6	-1.342372	0.477757	4.085194
6	-0.881134	0.947866	2.862933
7	-0.581412	0.120741	1.849103
78	0.111743	0.685420	-0.017741
17	0.159105	3.174286	0.308482
1	-0.038163	-5.033509	-0.756243
1	-1.570074	1.179161	4.879541
9	-0.787659	-4.231265	1.579334
9	0.765404	-3.704375	-2.817797
1	1.781759	2.324031	-4.661692
6	-1.994401	-1.445391	5.574771
1	-1.302788	-2.824086	3.329137
1	1.346905	-1.926524	-4.160305
6	2.066929	-0.058477	-6.007435
1	1.018880	2.595107	-2.289373
1	-0.737077	2.002677	2.660642
6	-1.074893	-1.962969	6.506533
6	-1.557504	-2.471259	7.716051
6	-2.922445	-2.480169	8.019076
6	-2.922445	-2.480169	8.019076
6	-3.814376	-1.966767	7.072517
6	-3.374256	-1.444178	5.852881
6	0.407616	-1.967470	6.215074
1	-0.848723	-2.869970	8.438230
6	-3.418255	-3.007587	9.343707
1	-4.880774	-1.974496	7.286217
6	-4.368420	-0.905172	4.851000

1	-4.225963	0.168073	4.677637
1	-4.264303	-1.398237	3.877360
1	-5.393425	-1.055989	5.200784
1	-4.431480	-3.413179	9.257477
1	-2.763638	-3.795443	9.730278
1	-3.449253	-2.210542	10.098216
1	0.972501	-2.330530	7.078121
1	0.649530	-2.609741	5.359952
1	0.771176	-0.963207	5.967956
6	3.418074	0.134761	-6.356941
6	3.809174	-0.089384	-7.679958
6	2.896564	-0.486401	-8.662032
6	1.562199	-0.671647	-8.288752
6	1.128878	-0.468572	-6.975320
6	4.442662	0.551788	-5.326892
1	4.854381	0.046436	-7.948301
6	3.336076	-0.685022	-10.092291
1	0.837796	-0.981868	-9.038310
6	-0.325727	-0.675967	-6.620172
1	5.453185	0.488794	-5.740160
1	4.284664	1.583125	-4.990056
1	4.398003	-0.082783	-4.434581
1	2.705719	-1.418201	-10.605649
1	3.271120	0.253985	-10.657597
1	4.375191	-1.025565	-10.146891
1	-0.467277	-1.558180	-5.984551
1	-0.731797	0.179552	-6.068952
1	-0.927283	-0.817244	-7.522438

[Pt(bis(4-Mes-py)-4,6-dFb)Cl] dimer (B3LYP/6-31G/CPCM-CH₂Cl₂)**

138

6	17.564879	0.624310	5.110732
6	16.451211	0.644947	5.948683
7	15.220129	1.008110	5.446079
6	15.098058	1.346347	4.153949
6	16.176427	1.323463	3.284902
6	17.445449	0.955139	3.754060
6	16.425268	0.329707	7.381892
6	17.459765	-0.062014	8.234772
6	17.255861	-0.284414	9.594882
6	15.985763	-0.090225	10.129559
6	14.898941	0.300107	9.343038
6	15.162255	0.488854	7.975392
9	15.836908	-0.260767	11.463422

9	18.716547	-0.199004	7.758311
78	13.704337	1.048704	6.849456
17	11.799733	1.752406	5.374862
6	13.509336	0.580070	9.719844
7	12.714693	0.946710	8.655027
6	11.421765	1.243759	8.854203
6	10.839344	1.181637	10.109879
6	11.612749	0.811684	11.218822
6	12.964821	0.518906	11.000993
6	10.988813	0.708461	12.562887
6	10.352977	1.831853	13.129222
6	9.683234	1.684957	14.346345
6	9.638163	0.466430	15.023941
6	18.583620	0.886082	2.800933
6	18.923458	2.011786	2.021437
6	19.886962	1.876172	1.017469
6	20.517330	0.660752	0.758873
6	18.297627	3.374030	2.226473
6	10.395492	3.195713	12.477555
7	17.357649	2.700797	11.485679
6	17.479746	2.362602	12.777823
6	16.401491	2.385969	13.646983
6	15.132561	2.754810	13.177956
6	15.013059	3.085407	11.821238
6	16.126638	3.064263	10.983158
78	18.873422	2.660104	10.082286
17	20.777978	1.956084	11.556830
6	13.994666	2.824758	14.131351
6	13.333890	4.058122	14.345221
6	12.387578	4.146502	15.366496
6	12.061547	3.051737	16.173780
6	12.691172	1.835881	15.915368
6	13.654350	1.699445	14.911213
6	16.152570	3.379451	9.549931
6	17.415574	3.220242	8.956413
6	17.678937	3.409166	7.588795
6	16.592150	3.799672	6.802314
6	15.322047	3.993830	7.336991
6	15.118106	3.771298	8.697075
6	13.648914	5.295719	13.535159

6	11.046009	3.190531	17.279542
6	14.279398	0.336822	14.706348
6	19.068580	3.129342	7.211992
7	19.863147	2.762399	8.276765
6	21.156121	2.465514	8.077632
6	21.738722	2.528244	6.822071
6	20.965436	2.898644	5.713194
6	19.613263	3.191050	5.930939
6	21.589513	3.002854	4.369279
6	22.226295	1.880206	3.802527
6	22.895964	2.028129	2.585479
6	22.940104	3.246954	1.908370
6	22.285331	4.342402	2.480196
6	21.610374	4.246474	3.698647
6	22.185089	0.516037	4.453640
6	20.963909	5.484646	4.279792
6	23.645923	3.381029	0.582169
9	16.741053	3.970463	5.468491
9	13.861320	3.908289	9.173528
1	14.494308	4.270343	6.697502
1	18.083624	-0.560825	10.234382
1	18.477987	2.084691	13.094693
1	14.099766	1.623981	3.836994
1	16.551623	2.130606	14.688989
1	16.026324	1.578922	2.242914
1	14.053702	3.357098	11.405782
1	18.524301	0.352965	5.526240
1	11.902703	5.103032	15.548447
1	20.151360	2.749226	0.426566
1	12.426397	0.963131	16.506549
1	13.255969	6.186020	14.034232
1	19.066197	4.149186	2.147764
1	14.725368	5.432419	13.390935
1	17.541193	3.587774	1.460862
1	13.194581	5.255503	12.537809
1	17.807420	3.473773	3.196400
1	10.034257	3.311728	16.874586
1	11.039266	2.309723	17.928151
1	13.510704	-0.438014	14.786929
1	14.767915	0.236128	13.735668

1	15.037067	0.123448	15.470841
1	21.710991	2.184838	8.964889
1	10.866797	1.524130	7.966911
1	22.793231	2.306078	6.712653
1	9.784878	1.403981	10.219361
1	18.979283	3.468661	5.102623
1	13.598980	0.241537	11.829249
1	22.314486	5.303791	1.972235
1	9.194507	2.553375	14.780152
1	23.385429	1.160281	2.151358
1	19.873876	5.471580	4.163540
1	11.353769	3.378734	11.983771
1	21.169301	5.589798	5.349971
1	9.610848	3.317134	11.720952
1	21.333913	6.379909	3.772073
1	10.253320	3.975555	13.230195
1	24.232390	4.305166	0.533514
1	24.318050	2.537186	0.399618
1	22.924438	3.412877	-0.244107
1	22.970996	0.394525	5.208930
1	21.227678	0.332478	4.948864
1	22.326354	-0.263410	3.700416
6	10.292124	-0.629744	14.452577
6	10.967117	-0.534832	13.234059
6	8.932250	0.333416	16.350203
1	8.344516	-0.589912	16.398961
1	9.653745	0.300634	17.176433
1	8.261288	1.178188	16.532732
1	10.262297	-1.590889	14.960963
6	11.612858	-1.773624	12.653456
1	12.702910	-1.761004	12.769592
1	11.242473	-2.668457	13.161657
1	11.407299	-1.879202	11.583350
6	20.191792	-0.434403	1.565849
6	19.245225	-0.346829	2.586944
6	18.930788	-1.584802	3.396660
1	19.324465	-2.474738	2.897515
1	19.384799	-1.544490	4.394150
1	17.854380	-1.722244	3.540539

1	20.677278	-1.390599	1.383769
6	21.533021	0.522726	-0.346848
1	21.326242	-0.356674	-0.967306
1	21.540005	1.404075	-0.994717
1	22.544688	0.400964	0.058135
1	11.252678	4.070509	17.899209

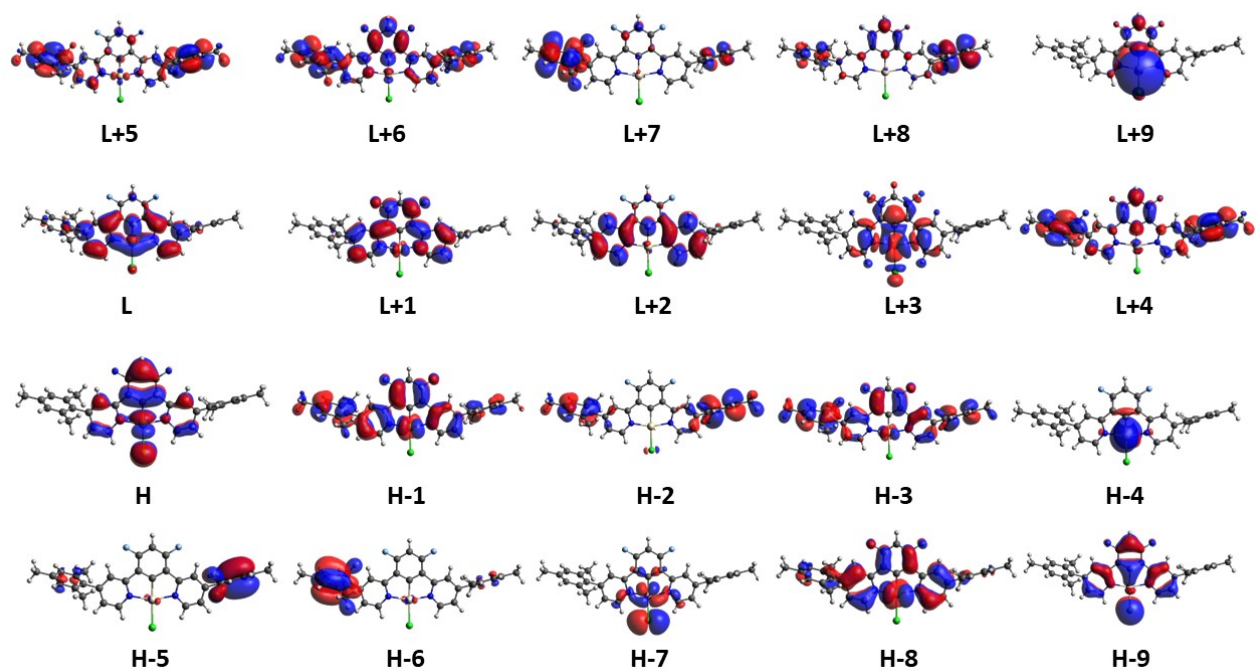


Figure S19. Isodensity plots (isodensity contour=0.02) of frontier molecular orbitals of **[Pt(bis(4-Mes-py)-4,6-dFb)Cl]** from the HOMO-9 to the LUMO+9.

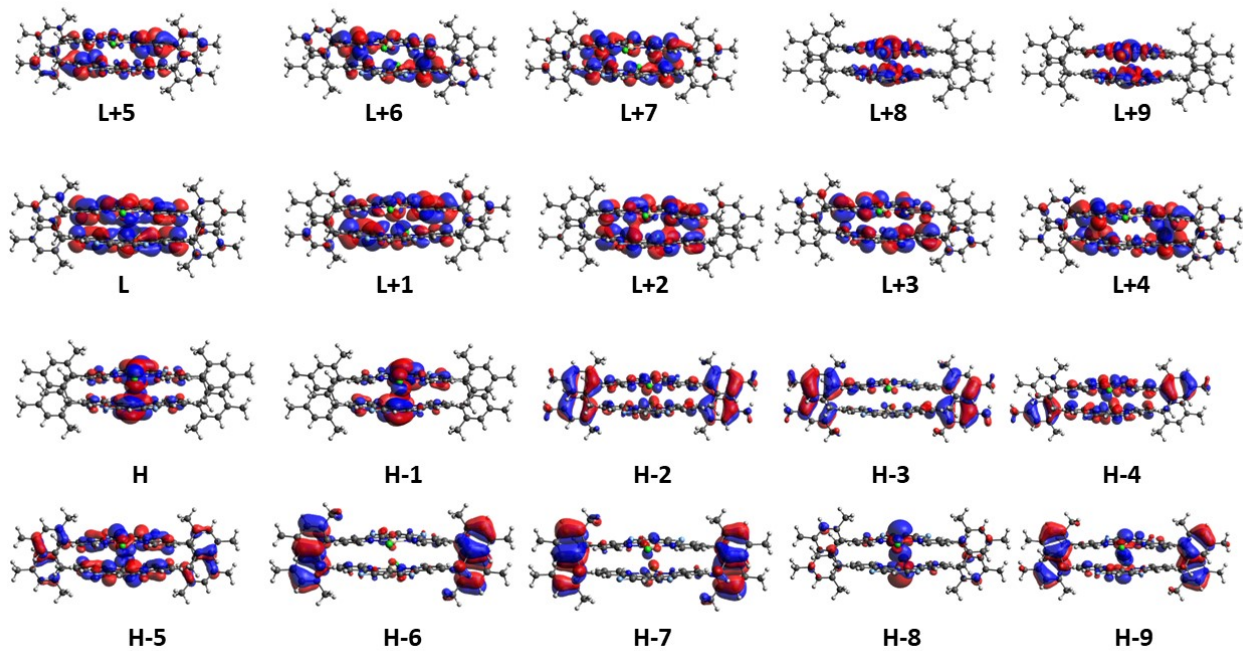


Figure S20. Isodensity plots (isodensity contour=0.02) of frontier molecular orbitals of the **[Pt(bis(4-Mes-py)-4,6-dFb)Cl]** dimer from the HOMO-9 to the LUMO+9.

Table S3: Computed singlet-singlet excitation energies (eV) and λ (nm), oscillator strength (f) and character of the singlet excited states of **[Pt(bis(4-Mes-py)-4,6-dFb)Cl]**.

Excited States ^a	E(eV)/ λ (nm)	f (oscillator strength)	Character ^b
S ₀ →S ₁	3.31 eV / 375 nm	0.01	96%(H→L)
S ₀ →S ₂	3.40 eV / 365 nm	0.17	94%(H→L+1)
S ₀ →S ₄	3.55 eV / 349 nm	0.06	78%(H-1→L); 13%(H-3→L)
S ₀ →S ₆	3.81 eV / 326 nm	0.12	36%(H-3→L); 22%(H-2→L); 10%(H-1→L+1); 6%(H-1→L); 5%(H-3→L+1)
S ₀ →S ₇	3.82 eV / 325 nm	0.09	29%(H-3→L); 29%(H-2→L); 18%(H-2→L+1); 13%(H-7→L)
S ₀ →S ₉	3.98 eV / 312 nm	0.05	56%(H-1→L+1); 11%(H-8→L+1); 9%(H-6→L); 8%(H-2→L)
S ₀ →S ₁₂	4.09 eV / 303 nm	0.03	75%(H-7→L+1); 12%(H-2→L+1)
S ₀ →S ₁₃	4.12 eV / 301 nm	0.20	52%(H-8→L); 17%(H→L+2); 13%(H-7→L+1); 7%(H-2→L+1)
S ₀ →S ₁₅	4.18 eV / 297 nm	0.03	54%(H-3→L+1); 10%(H-2→L+1); 5%(H-3→L)
S ₀ →S ₁₆	4.22 eV / 294 nm	0.18	66%(H→L+2); 24%(H-8→L)
S ₀ →S ₂₀	4.37 eV / 284 nm	0.06	56%(H-8→L+1); 16%(H-1→L+2); 10%(H-9→L)
S ₀ →S ₂₁	4.41 eV / 281 nm	0.07	80%(H→L+3); 5%(H-9→L)
S ₀ →S ₂₃	4.55 eV / 273 nm	0.04	49%(H-9→L); 25%(H-4→L+2); 17%(H-4→L+4)
S ₀ →S ₂₆	4.65 eV / 267 nm	0.13	44%(H-1→L+2); 11%(H-3→L+2); 8%(H-9→L+1); 7%(H-2→L+3); 7%(H-1→L+3)
S ₀ →S ₂₇	4.68 eV / 265 nm	0.15	51%(H-2→L+2); 15%(H-2→L+3); 12%(H-1→L+3)
S ₀ →S ₃₀	4.77 eV / 260 nm	0.11	21%(H-1→L+3); 19%(H-7→L+4); 17%(H-3→L+2); 10%(H-2→L+3)

			1→L+2)
S ₀ →S ₃₂	4.82 eV / 257 nm	0.12	72%(H-7→L+2); 10%(H-10→L)
S ₀ →S ₃₃	4.83 eV / 257 nm	0.02	63%(H-6→L+2); 19%(H-6→L+3)
S ₀ →S ₃₅	4.84 eV / 256 nm	0.04	79%(H-10→L); 7%(H-7→L+2)
S ₀ →S ₃₆	4.86 eV / 253 nm	0.47	31%(H-7→L+2); 14%(H-1→L+3); 17%(H-7→L+2); 9%(H-3→L+3)
S ₀ →S ₄₀	5.10 eV / 243 nm	0.04	48%(H-3→L+3); 25%(H-2→L+2); 14%(H-2→L+3); 5%(H-1→L+3)

^a The reported excited states are characterized by $f \geq 0.02$, except S₀→S₁ that as the lowest state is reported and discussed

^b Only the components $\geq 5\%$ are reported in the Excited state character

Table S4. Computed singlet-singlet excitation energies (eV) and λ (nm), oscillator strength (f) and character of the singlet excited states of the [Pt(bis(4-Mes-py)-4,6-dFb)Cl] dimer.

Excited States ^a	E(eV)/ λ (nm)	f (oscillator strength)	Character ^b
S ₀ →S ₁	3.05 eV / 407 nm	0.03	95%(H→L)
S ₀ →S ₄	3.24 eV / 383 nm	0.17	94%(H→L+2)
S ₀ →S ₆	3.35 eV / 371 nm	0.02	63%(H-1→L+1); 23%(H-8→L)
S ₀ →S ₉	3.43 eV / 361 nm	0.02	36%(H-4→L); 31%(H-1→L+3); 8%(H-2→L+1)
S ₀ →S ₁₀	3.47 eV / 358 nm	0.37	56%(H-1→L+3); 22%(H-4→L); 6%(H-2→L+1)
S ₀ →S ₁₂	3.60 eV / 345 nm	0.02	73%(H-3→L); 10%(H-2→L+3); 5%(H-4→L)
S ₀ →S ₁₄	3.63 eV / 342 nm	0.07	46%(H-8→L); 24%(H-1→L+1); 8%(H-2→L+1)
S ₀ →S ₁₆	3.70 eV / 335 nm	0.33	49%(H-2→L+1); 16%(H-3→L+2); 12%(H-4→L); 7%(H-13→L); 5%(H-2→L+3)
S ₀ →S ₁₇	3.75 eV / 330 nm	0.23	40%(H-5→L+1); 9%(H-4→L); 6%(H-6→L+1); 5%(H-7→L); 5%(H-2→L+3); 5%(H-3→L+3)
S ₀ →S ₂₂	3.79 eV / 327 nm	0.02	56%(H-15→L); 18%(H-14→L+1); 6%(H-4→L+2)
S ₀ →S ₂₄	3.80 eV / 326 nm	0.03	51%(H-7→L); 8%(H-4→L+2); 8%(H-5→L+1); 7%(H-3→L+2); 7%(H-6→L+3)
S ₀ →S ₂₅	3.81 eV / 325 nm	0.06	49%(H-2→L+3); 14%(H-7→L); 7%(H-3→L); 6%(H-4→L); 6%(H-2→L+1)
S ₀ →S ₂₆	3.84 eV / 323 nm	0.15	23%(H-4→L+2); 18%(H-10→L); 14%(H-8→L+2); 8%(H-3→L+2); 7%(H-9→L+3); 6%(H-6→L+1); 5%(H-7→L)
S ₀ →S ₃₂	3.94 eV / 314 nm	0.03	29%(H-3→L+2); 14%(H-11→L+1); 11%(H-5→L+1); 9%(H-4→L+2); 7%(H-2→L+1); 5%(H-6 L+1)
S ₀ →S ₃₅	3.96 eV / 313 nm	0.14	23%(H-13→L); 15%(H-3→L+2); 13%(H-5→L+3); 9%(H-8→L+2); 9%(H-6→L+1); 7%(H-7→L+2); 5%(H-11→L+3); 5%(H→L+5)
S ₀ →S ₃₆	3.96 eV / 313 nm	0.03	24%(H-5→L+3); 19%(H-13→); 8%(H-6→L+1); 7%(H-8→L+2); 6%(H-4→L+2); 6%(H-11→L+3)
S ₀ →S ₃₈	3.99 eV / 311 nm	0.03	27%(H-1→L+1); 21%(H-9→L+1); 11%(H-3→L+2); 8%(H-8→L); 5%(H-4→L+2); 5%(H-11→L+3)
S ₀ →S ₄₀	4.01 eV / 309 nm	0.03	22%(H-6→L+1); 20%(H-13→L); 19%(H-10→L); 19%(H-7→L+2);
S ₀ →S ₄₆	4.07 eV / 305 nm	0.09	50%(H→L+5); 13%(H-9→L+1); 5%(H-13→L)

$S_0 \rightarrow S_{51}$	4.15 eV / 299 nm	0.03	25%(H→L+6); 22%(H-6→L+3); 17%(H-13→L+2); 12%(H-12→L+1); 5%(H-6→L+1)
$S_0 \rightarrow S_{52}$	4.15 eV / 299 nm	0.03	40%(H→L+6); 28%(H-6→L+3); 6%(H-12→L+1); 5%(H-5→L+3)
$S_0 \rightarrow S_{57}$	4.18 eV / 297 nm	0.08	22%(H-6→L+3); 19%(H-12→L+1); 14%(H-7→L+2); 9%(H-13→L+2); 7%(H-17→L); 6%(H→L+6)
$S_0 \rightarrow S_{58}$	4.21 eV / 294 nm	0.05	37%(H-17→L); 12%(H-16→L+1); 7%(H-13→L+2); 6%(H-12→L+3); 5%(H-11→L+3)
$S_0 \rightarrow S_{60}$	4.23 eV / 293 nm	0.06	30%(H-10→L+3); 15%(H-9→L+1); 9%(H-2→L+1); 7%(H-12→L+1); 5%(H-13→L+2)
$S_0 \rightarrow S_{76}$	4.36 eV / 284 nm	0.02	30%(H-12→L+3); 21%(H-12→L+1); 15%(H-13→L+2); 10%(H-2→L+4); 6%(H-16→L+1)
$S_0 \rightarrow S_{79}$	4.40 eV / 282 nm	0.08	20%(H-16→L+1); 18%(H-16→L+3); 11%(H-2→L+4); 11%(H-17→L); 6%(H-1→L+9); 6%(H-5→L+4); 5%(H-3→L+6); 6%(H-17→L+2)
$S_0 \rightarrow S_{85}$	4.51 eV / 275 nm	0.02	26%(H-5→L+4); 14%(H-19→L); 12%(H-1→L+7); 9%(H-8→L+5); 9%(H-16→L+3); 6%(H-11→L+4)
$S_0 \rightarrow S_{86}$	4.52 eV / 274 nm	0.11	33%(H-17→L+2); 13%(H-19→L); 11%(H-16→L+3); 7%(H-18→L+3); 6%(H-4→L+6)
$S_0 \rightarrow S_{88}$	4.53 eV / 274 nm	0.28	35%(H-19→L); 12%(H-16→L+1); 10%(H-1→L+7); 7%(H-4→L+6)
$S_0 \rightarrow S_{90}$	4.53 eV / 273 nm	0.08	38%(H-1→L+7); 19%(H-5→L+4); 9%(H-8→L+6)
$S_0 \rightarrow S_{91}$	4.54 eV / 273 nm	0.38	29%(H-17→L+2); 18%(H-4→L+5); 6%(H-18→L); 6%(H-11→L+4); 5%(H-3→L+5)
$S_0 \rightarrow S_{94}$	4.60 eV / 269 nm	0.05	23%(H-3→L+5); 15%(H-11→L+4); 9%(H-9→L+4); 7%(H-16→L+3); 6%(H-17→L+2); 6%(H-5→L+4); 6%(H-8→L+5)
$S_0 \rightarrow S_{97}$	4.63 eV / 268 nm	0.03	52%(H-6→L+4); 18%(H-4→L+5); 11%(H-18→L+3); 10%(H-19→L+2); 7%(H-6→L+4); 6%(H-17→L+2)
$S_0 \rightarrow S_{100}$	4.66 eV / 266 nm	0.15	25%(H-18→L+1); 18%(H-4→L+5); 11%(H-18→L+3); 10%(H-19→L+2); 7%(H-6→L+4); 6%(H-17→L+2)
$S_0 \rightarrow S_{102}$	4.68 eV / 265 nm	0.08	31%(H-4→L+6); 15%(H-4→L+5); 9%(H-18→L+1); 8%(H-3→L+5); 7%(H-3→L+6)
$S_0 \rightarrow S_{107}$	4.73 eV / 262 nm	0.15	32%(H-18→L+3); 20%(H-18→L+1); 10%(H-3→L+6); 5%(H-19→L)
$S_0 \rightarrow S_{109}$	4.74 eV / 261 nm	0.02	19%(H-1→L+7); 18%(H-8→L+6); 17%(H-8→L+5); 8%(H-3→L+6); 8%(H-4→L+6); 8%(H-18→L+3)
$S_0 \rightarrow S_{113}$	4.77 eV / 260 nm	0.08	43%(H-19→L+2); 10%(H-18→L+3); 8%(H-8→L+6); 6%(H-3→L+6); 5%(H-18→L+1); 5%(H-4→L+6)
$S_0 \rightarrow S_{117}$	4.80 eV / 258 nm	0.02	21%(H-8→L+6); 15%(H-9→L+4); 13%(H-7→L+5); 12%(H-8→L+5); 5%(H-19→L+2); 5%(H-2→L+7)
$S_0 \rightarrow S_{126}$	4.87 eV / 255 nm	0.05	22%(H-2→L+5); 22%(H-12→L+4); 10%(H-13→L+6); 7%(H-3→L+5); 6%(H-5→L+7); 5%(H-4→L+5)
$S_0 \rightarrow S_{128}$	4.89 eV / 254 nm	0.18	33%(H-10→L+5); 11%(H-15→L+8); 11%(H-14→L+9); 7%(H-2→L+7); 5%(H-6→L+4)
$S_0 \rightarrow S_{129}$	4.90 eV / 253 nm	0.09	28%(H-10→L+5); 15%(H-12→L+4); 7%(H-15→L+8); 7%(H-14→L+9)
$S_0 \rightarrow S_{132}$	4.95 eV / 250 nm	0.09	49%(H-15→L+6); 13%(H-14→L+7); 11%(H-15→L+5); 5%(H-15→L+8)
$S_0 \rightarrow S_{134}$	4.98 eV / 249 nm	0.02	61%(H-7→L+6); 14%(H-6→L+4); 5%(H-10→L+6)
$S_0 \rightarrow S_{136}$	5.00 eV / 248 nm	0.10	41%(H-5→L+7); 23%(H-3→L+5); 11%(H-2→L+7)
$S_0 \rightarrow S_{137}$	5.00 eV / 248 nm	0.03	41%(H-13→L+5); 20%(H-5→L+7); 5%(H-2→L+7)
$S_0 \rightarrow S_{139}$	5.03 eV / 246 nm	0.02	40%(H-22→L); 25%(H→L+10); 17%(H-16→L+4)

$S_0 \rightarrow S_{140}$	5.04 eV / 246 nm	0.13	46%(H-10→L+6); 11%(H-9→L+4); 11%(H-13→L+6); 8%(H-8→L+6)
$S_0 \rightarrow S_{145}$	5.06 eV / 245 nm	0.14	41%(H→L+10); 35%(H-22→L)
$S_0 \rightarrow S_{146}$	5.08 eV / 244 nm	0.04	40%(H-16→L+4); 9%(H-15→L+5); 8%(H-24→L); 7%(H→L+10)

^a The reported excited states are characterized by $f \geq 0.02$

^b Only the components $\geq 5\%$ are reported in the Excited state character

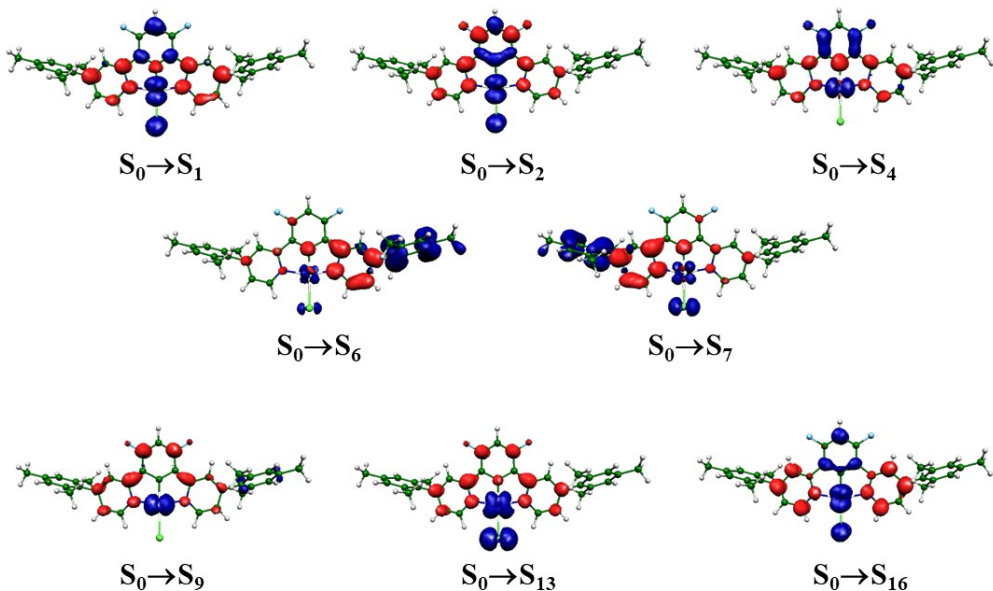


Figure S21. Isodensity difference plots of the lowest energy $S_0 \rightarrow S_n$ excitations with a significant oscillator strength ≥ 0.05 of $[\text{Pt}(\text{bis}(4\text{-Mes-py})\text{-}4,6\text{-dFb})\text{Cl}]$ (isodensity plot contour=0.02).

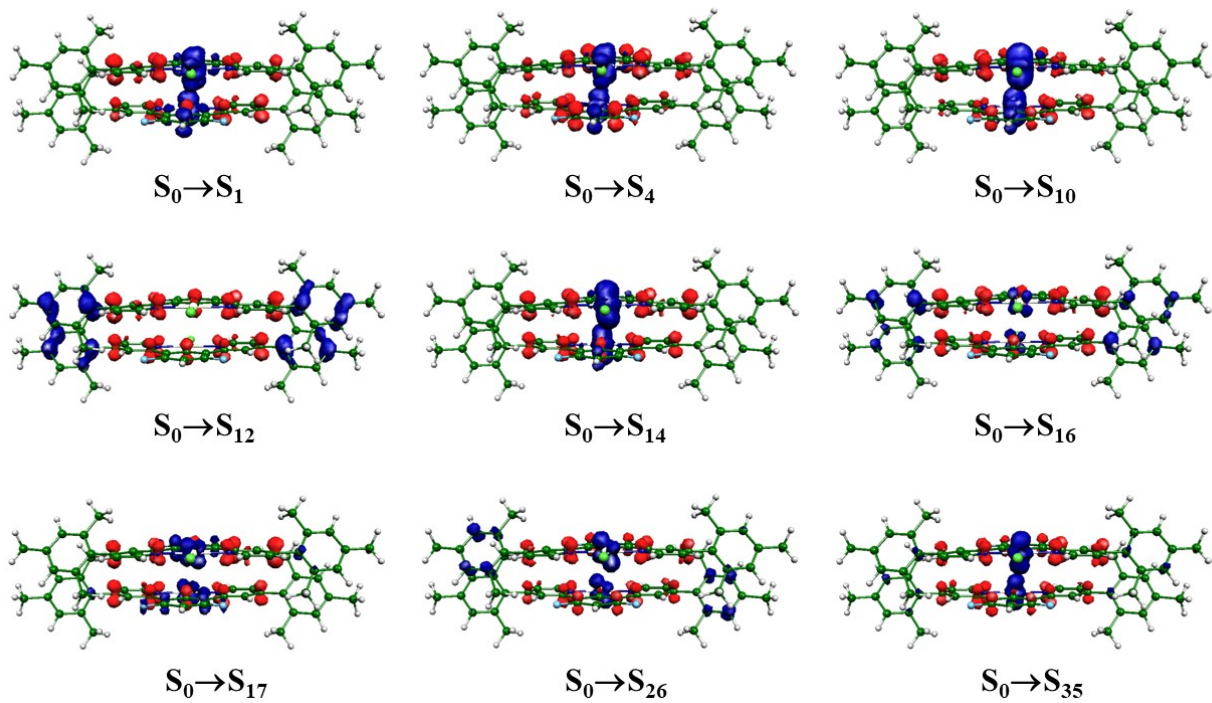


Figure S22. Isodensity difference plots of the lowest energy $S_0 \rightarrow S_n$ excitations with a significant oscillator strength, $0.14 \leq f \leq 0.37$ of the $[\text{Pt}(\text{bis}(4\text{-Mes-py})\text{-}4,6\text{-dFb})\text{Cl}]$ dimer (isodensity plot contour=0.02).

Table S5. The lowest 5 computed singlet-triplet excitation energies (eV) and λ (nm) for $[\text{Pt}(\text{bis}(4\text{-Mes-py})\text{-}4,6\text{-dFb})\text{Cl}]$ (B3LYP-LANL2DZ/6-31G**/CPCM).

Excited States	E(eV)/ λ (nm)
$S_0 \rightarrow T_1$	2.73 eV / 453 nm
$S_0 \rightarrow T_2$	2.97 eV / 417 nm
$S_0 \rightarrow T_3$	3.09 eV / 401 nm
$S_0 \rightarrow T_4$	3.23 eV / 383 nm
$S_0 \rightarrow T_5$	3.35 eV / 370 nm

Table S6. The lowest 10 computed singlet-triplet excitation energies (eV) and λ (nm) for the $[\text{Pt}(\text{bis}(4\text{-Mes-py})\text{-}4,6\text{-dFb})\text{Cl}]$ dimer (B3LYP-LANL2DZ/6-31G**/CPCM).

Excited States	E(eV)/ λ (nm)
$S_0 \rightarrow T_1$	2.63 eV / 471 nm
$S_0 \rightarrow T_2$	2.70 eV / 459 nm
$S_0 \rightarrow T_3$	2.87 eV / 431 nm
$S_0 \rightarrow T_4$	2.89 eV / 429 nm
$S_0 \rightarrow T_5$	2.97 eV / 418 nm
$S_0 \rightarrow T_6$	3.02 eV / 410 nm
$S_0 \rightarrow T_7$	3.08 eV / 403 nm
$S_0 \rightarrow T_8$	3.08 eV / 402 nm
$S_0 \rightarrow T_9$	3.12 eV / 397 nm
$S_0 \rightarrow T_{10}$	3.17 eV / 391 nm

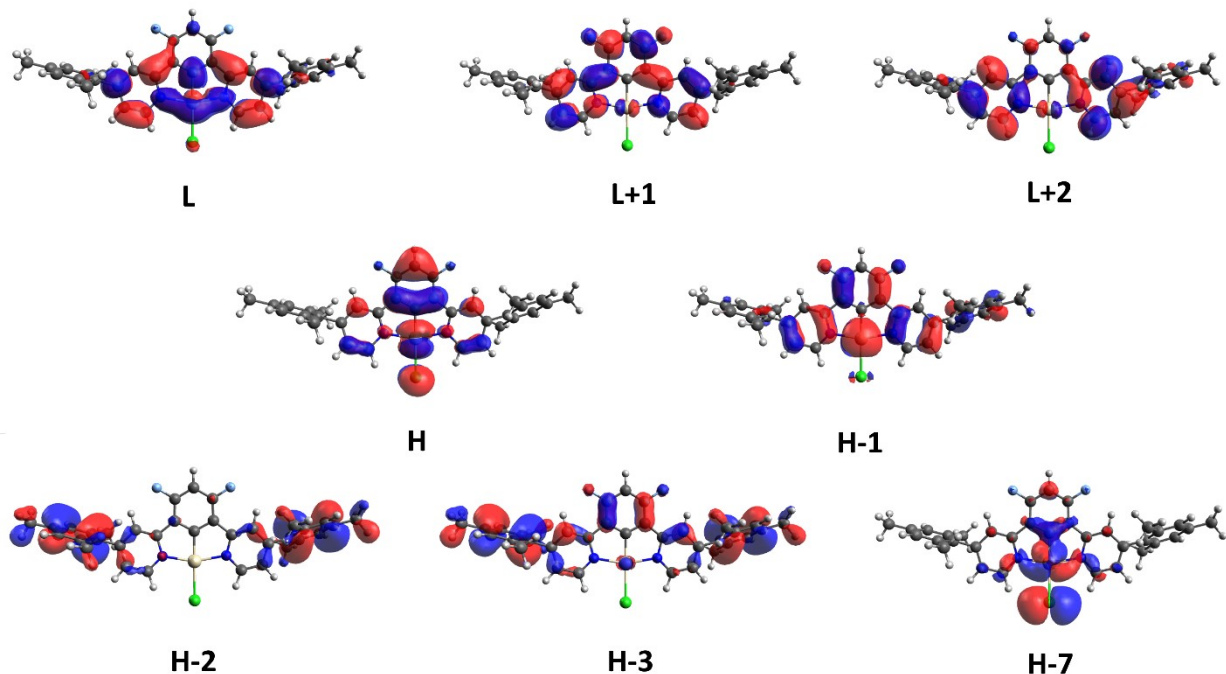


Figure S23. Isodensity plots (isodensity contour=0.02) of SOC frontier molecular orbitals of **[Pt(bis(4-Mes-py)-4,6-dFb)Cl]** mostly involved in the absorption spectrum transitions.

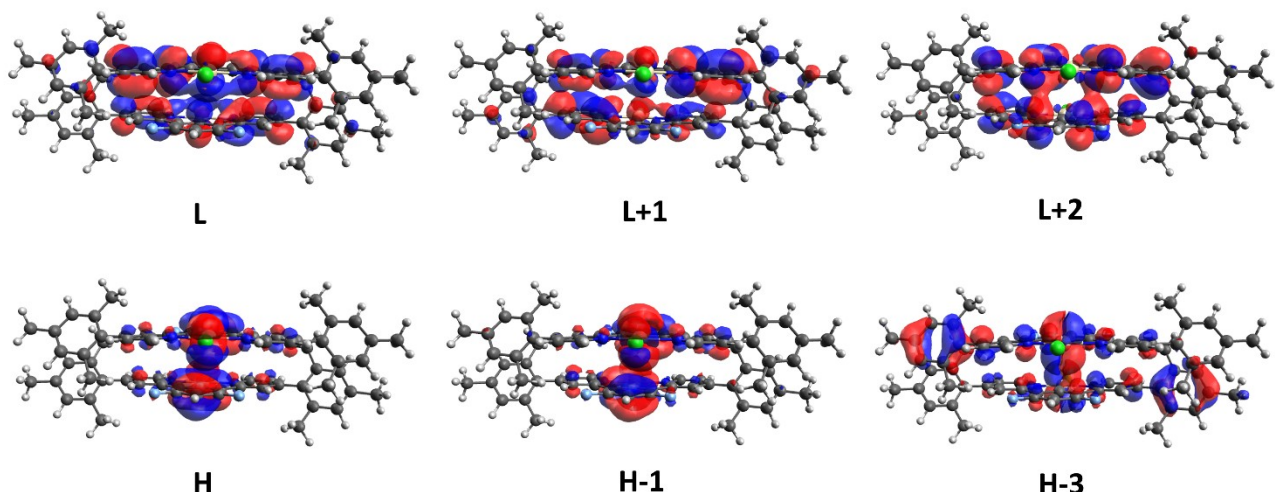


Figure S24. Isodensity plots (isodensity contour=0.02) of SOC frontier molecular orbitals of the **[Pt(bis(4-Mes-py)-4,6-dFb)Cl]** dimer mostly involved in the absorption spectrum transitions.

VII. OLEDs fabrication

OLEDs were fabricated by growing a sequence of thin layers on clean glass substrates pre-coated with a 120 nm-thick layer of indium tin oxide (ITO) with a sheet resistance of 20 U per square. A 2 nm-thick hole-injecting layer of MoO_x was deposited on top of the ITO by thermal evaporation under high vacuum of 10⁻⁶ hPa. The other layers were deposited in succession by thermal evaporation under high vacuum: first, 4,4',4''-tris(N-carbazolyl)triphenylamine (TCTA, 50 nm) as exciton blocking layers; second, the emitting layer (EML) evaporated by co-deposition of [Pt(bis(4-Mes-py)-4,6-dFb)Cl] and (bis-4-(N-carbazolyl)phenyl)phenylphosphine oxide (BCPO) to form a 30 nm-thick blend film (8 wt% Pt complex : 92 wt% BCPO or 70 wt% Pt complex : 30 wt% BCPO), or by single deposition of only [Pt(bis(4-Mes-py)-4,6-dFb)Cl], to form a 30 nm neat film; third, 2,2',2''-(1,3,5-benzinetriyl)-tris(1-phenyl-1-H-benzimidazole (TPBi, 30 nm) as an electron-transporting and hole-blocking layer. This was followed by thermal evaporation of the cathode layer consisting of 0.5 nm thick LiF and a 100 nm thick aluminium cap.

The current–voltage characteristics were measured with a Keithley Source-Measure unit, model 236, under continuous operation mode, while the light output power was measured with an EG&G power meter, and electroluminescence (EL) spectra recorded with a StellarNet spectroradiometer. All measurements were carried out at room temperature under argon atmosphere and were reproduced for many runs, excluding any irreversible chemical and morphological changes in the devices.

VIII. References

- [1] F. Henwood, A. K. Bansal, D. B. Cordes, A. M. Z. Slawin, I. D. W. Samuel and E. Zysman-Colman, *J. Mater. Chem. C*, 2016, **4**, 3726.
- [2] L. Murphy, P. Brulatti, V. Fattori, M. Cocchi and J. A. G. Williams, *Chem. Commun.*, 2012, 48, 5817.
- [3] K. Suzuki, A. Kobayashi, S. Kaneko, K. Takehira, T. Yoshihara, H. Ishida, Y. Shiina, S. Oishic and S. Tobita, *Phys. Chem. Chem. Phys.*, 2009, **11**, 9850–9860.